RIB Physics with Storage Rings

Script of the lecture given at the EJC2015 school on "Instrumentation, detection, and simulation in modern nuclear physics"

Yuri A. Litvinov

GSI Helmholtzzentrum für Schwerionenforschung, Plankstraße 1, 64291 Darmstadt, Germany

Abstract

In the last two decades a number of nuclear structure and astrophysics experiments were performed at heavy-ion storage rings employing unique experimental conditions offered by such machines. Furthermore, building on the experience gained at the facilities presently in operation, several new storage ring projects were launched worldwide. This skript is intended to provide a brief review of the fast growing field of nuclear structure and astrophysics research at storage rings. The material for this script is partially taken from recent publications, lectures and reviews by my colleagues to whom I am deeply obliged.

It is emphasized that the script uses material which is published in Refs. [8, 26, 47, 13, 43, 22, 100]

Contents

1 Introduction

Heavy-ion storage rings coupled to radioactive ion beam facilities offer unique capabilities for nuclear physics experiments. There are presently three operational facilities, namely the Experimental Storage Ring (ESR) at GSI in Darmstadt, Germany, the experimental Cooler-Storage Ring (CSRe) at IMP in Lanzhou, P. R. China, and the Rare-RI Storage Ring (R3) at RIKEN in Wako, Japan, at which several research programs are being pursued [100].

Well-established are direct mass measurements of short-lived nuclei, see Section 6. A characteristic property of the storage ring mass spectrometry is that masses of several tens of isotopes can be measured in a single experiment. Nuclei with half-lives as short as a few ten microseconds can be addressed, which, together with the sensitivity to single stored ions, allows addressing the most exotic nuclear species [26].

Owing to the ultra-high vacuum conditions, high atomic charge states of stored ions can be preserved for extended periods of time, which is the indispensable prerequisite for decay studies of highly-charged ions, see Section 7. One prominent example is the bound-state beta decay, which was discovered in the ESR. In the recent years, a lot of attention has been given to electron-capture decay of few-electron ions [47].

Storage rings are being considered for nuclear reaction studies, see Section 8 [43]. Compared to external target experiments, here a thin windowless internal gas target combined with high revolution frequencies of stored ions offer advantageous conditions for a range of experiments. For instance proton capture reaction on slowed-down to 10 MeV/u fully-ionized ^{95}Rh was measured. After this proof-of-principle experiment, a series of measurements is envisioned on $p-$ and α-capture reactions directly in the Gamow window of the astrophysical p-process. The first in-ring transfer reaction $^{20}\mathrm{Ne}(p,d)^{19}\mathrm{Ne}$ has been successfully studied in the ESR in October 2012. Furthermore, proton scattering on stored ^{58}Ni and ^{56}Ni beams was investigated at the ESR as a part of the EXL commissioning program.

Research programs at storage rings have proven their high discovery potential, which is clearly indicated by a number of new storage ring projects started around the world: TSR@ISOLDE at CERN, CRYRING@ESR at GSI, as well as new storage ring complexes at FAIR in Germany and at HIAF in China. In the lecture given at the EJC2015 school on “Instrumentation, detection, and simulation in modern nuclear physics” a review was given on the present nuclear physics research programs at storage rings illustrated by examples of recent results. Also addressed were the plans for new storage ring projects.

2 Production and separation of exotic nuclei[1]

An indispensable prerequisite for the experimental investigations of short-lived nuclei, is their production and cleaning from inevitable–more abundant–contaminations [28, 31]. Dependent on the type of experiment further manipulations on the secondary beam may be necessary. Possible ways for the production, separation and storing of highly-charged exotic ions are schematically presented in figure 1 [47]. To date only the option (a) is realized at operating radioactive-ion beam facilities. The option (e) will be enabled with CRYRING installed behind the ESR, see Section 9.2. The option (d) is being planned at CERN within the TSR@ISOLDE project, see Section 9.1.

A variety of nuclear reactions are used for the production of radioactive nuclei in different energy regions: fission, target spallation, projectile fragmentation, fusion, deep inelastic and nuclear transfer reactions [31]. Schematic illustration of fragmentation, Coulomb dissociation, and fusion reactions is given in Figure 2. Here, we sketch only three main production reactions which are relevant for in-ring experiments.

- **Spallation reactions.** Spallation is well-known from particle cascades due to interactions of high-energy cosmic rays with atoms of the Earth atmosphere [66]. If a light projectile with a high kinetic energy (from hundreds of A·MeV to several A·GeV) collides with a heavy target nucleus, it can lead to spallation [53]. In this process, the projectile transfers its energy to target nucleons leading to a cascade of nucleon-nucleon collisions and resulting in an emission of nucleons (predominantly neutrons) and light fragments (d, t, α, etc.). Similar to the fragmentation reaction, mostly neutron-deficient nuclides are produced in this reaction. For more details and experimental data see, e.g., Ref. [24].

- **Fragmentation reactions.** At relativistic energies (from a few tens to a few hundreds of A·MeV) heavy projectiles can be fragmented, that is, a number of nucleons can be removed from the projectile. In a simplified picture the part of the projectile overlapping with the target nucleus is suddenly cut off, leaving a highly excited fragment travelling nearly with the same velocity and nearly in the same direction as the projectile. The de-excitation of the fragment proceeds mainly by evaporating neutrons, thus yielding neutron-deficient nuclides [31].

[1] Material for this section is taken from Refs. [47, 13]

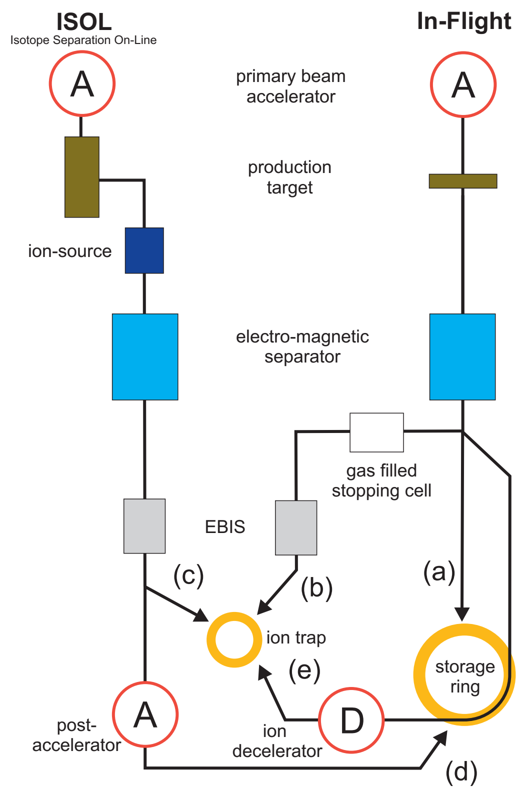

Fig. 1: Scenarios for production, separation and storage of highly-charged radioactive ions [47]. Both *Isotope Separation On-Line* (ISOL) and *in-flight* methods can be employed. In the latter case, the nuclides can be produced in the required high atomic charge state and can be directly stored in a high-energy storage ring (a). High-energy nuclides can be slowed down (and neutralized) in a gas catcher, then trapped in an *Electron-Beam Ion Trap/Source* (EBIS/EBIT) for charge breeding, extracted as highly-charged ions and stored in a dedicated ion trap (b). The ISOL beams can be trapped in an EBIS for charge breeding and subsequently stored at low energies in an ion trap (c). Another possibility is to re-accelerate the highly-charged ions from the EBIS and to store them in a storage ring (d). Option (e) is to slow down the highly-charged ions in a ring, extract them, further slow them down and finally store them in an ion trap. Taken from [49].

Many different nuclei can be created by removing nucleons from the projectile. Typically heavy-Z (Z is the proton number) projectiles and low-Z targets are used.

- **Fission.** Heavy nuclei near uranium can undergo fission, disintegrating most often into two fragments. Generally, stable heavy nuclei have more neutrons than protons and the neutron excess increases with the proton number. In fission the neutron-to-proton ratio stays nearly the same. Therefore, fission is a source of neutron-rich medium mass nuclei. In-flight fission induced by heavy- or light-Z target nuclei yields different mass-distributions of fission fragments [5, 23]. For example, ^{238}U fissions in the former case into two fragments with different masses (asymmetric fission), where one of the fragments is produced close to the doubly-magic ^{132}Sn nucleus. In the latter case a contribution due to the symmetric fission into two fragments with about equal masses becomes significant as well. In the centre-of-mass system the emission of fission fragments is isotropic and the energetics is determined by the Coulomb repulsion. In the case of uranium fission the total kinetic energy of the fragments is about 170 MeV.

The production rates of various fragments in the above reactions can quite reliably be described by modern reaction models. Such models typically calculate the probability to form an excited compound nucleus and its subsequent de-excitation. An example of measured and calculated cross-sections for the tin isotopic chain is shown in Figure 3 [26].

In principle, in all these reactions a huge number of nuclei are created. Therefore, a good separation is needed to extract the nuclides of interest from the unwanted contaminants. Two main complementary separation techniques exist which are briefly described below.

The Isotope Separation On-Line (ISOL) method is widely used for the production and the separation of radioactive nuclides.

Exotic nuclei are produced in a thick target (up to a few 100 g/cm^2) by bombarding it with protons or light ion beams at high energies (100-1000 MeV/u). The products of target spallation or fission reactions are stopped in the target-ion-source system.

After ionization the ions are extracted and accelerated up to a few tens keV. The singly-charged ions are then mass separated in electromagnetic fields. In this way isobaric contaminations are inevitable. An additional separation criterion can be introduced by applying a resonant laser ionization source [39]. This method provides a selection for different elements.

The yields of exotic nuclei at an ISOL-type facility are primarily determined by the intensity and the energy of the primary beam, production cross-section and target thickness. In addition the release processes from the target-ion-source system and transfer efficiency yield the rate at the detector system. The release precesses are strongly dependent on the chemical properties of produced nuclides, see Figure 4. For example, the alkalides are very efficiently extracted by ISOL-systems. The disadvantages are that not all chemical elements can be provided and that the extraction processes take at least a few milliseconds which restricts the nuclei which can be investigated.

Thus, the chemical properties and the nuclear half-lives play a crucial role in the production and the separation of exotic nuclei with the ISOL-method (see Figure 4). Typical examples of ISOL-type facilities are ISOLDE at CERN/Geneva (see Figure 5) and ISAC at TRIUMF/Vancouver. The new generation of ISOL-facilities are equipped with post-accelerators to allow

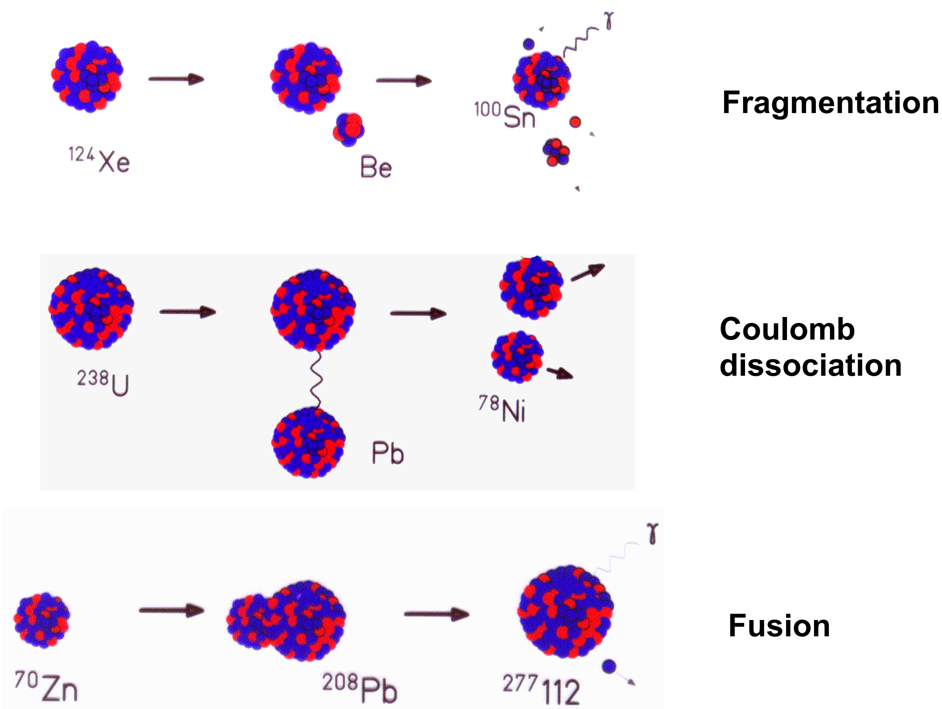

Fig. 2: Schematic illustration of fragmentation (top), Coulomb dissociation (middle), and fusion (bottom) reactions.

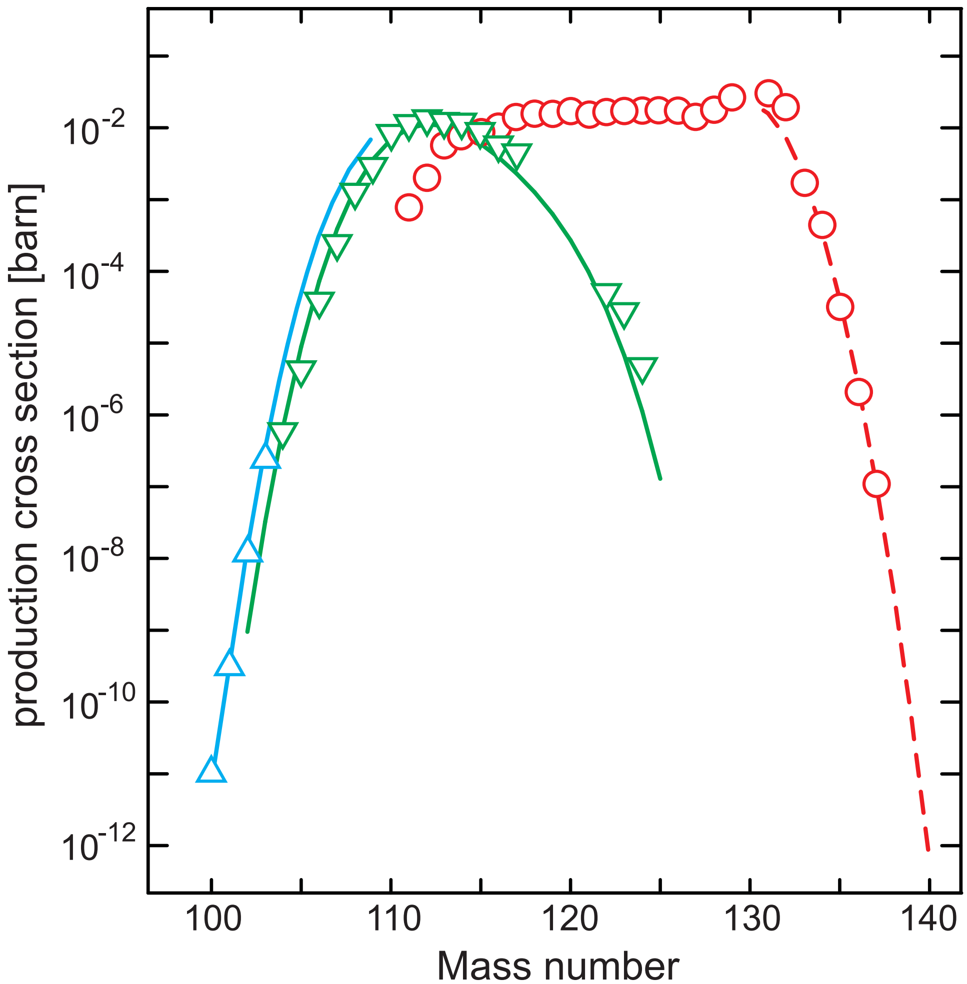

Fig. 3: Experimental (symbols) and calculated (lines) production cross-sections for the chain of tin isotopes. Considered here are the projectile fission reaction of ^{238}U ions (open circles), and the fragmentation reactions of ^{124}Xe (open upright triangles) and ^{129}Xe (open downward triangles) projectiles. The corresponding calculations with ABRABLA [27] and EPAX [76, 75] codes are shown with dashed and solid lines, respectively. The production rates for the spallation reactions on ^{124}Xe and ^{129}Xe targets are similar to the case of the fragmentation reaction. Taken from [13]. Courtesy to Hans Geissel.

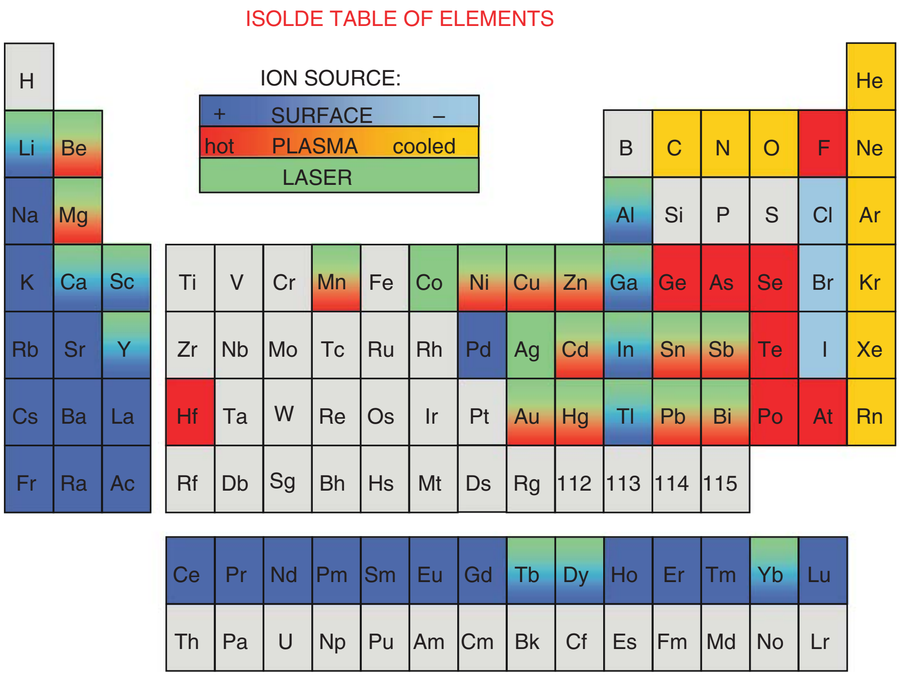

Fig. 4: Color coded periodic table of elements and the ion sources in use for their production at ISOLDE/CERN. Taken from Ref. [8]. Courtesy to Klaus Blaum.

nuclear reaction studies with radioactive beams. The pioneering facility of this development was built in Louvain-la-Neuve.

A complementary technique for rare isotope investigations is the in-flight separation method. All running storage ring facilities employ in flight separation technique. This method is used in a wide energy range of the projectiles, from the Coulomb barrier up to a few GeV/u. The projectiles impinge on a thin target which enables that the reaction products emerge with high kinetic energies. Fusion, projectile fragmentation, projectile fission and electromagnetic dissociation are the main production mechanisms. With these four mechanisms basically all nuclides below uranium can be produced [31].

Due to the kinematics of the reaction the products are mainly emitted in the forward direction. Depending on the energy range, the reaction products have characteristic charge state distributions [70]. The main advantage of high energies is that the fragments emerge from the target with only a

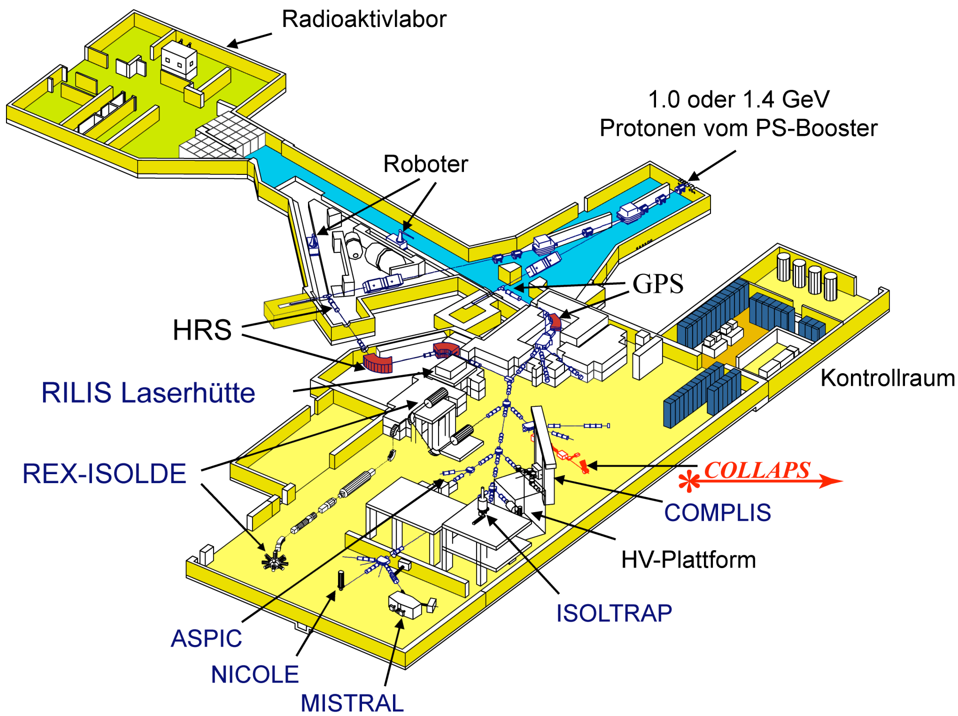

Fig. 5: A schematic view of ISOLDE facility at CERN. Courtesy to Klaus Blaum.

few electrons or fully ionized which allows an efficient electromagnetic separation in-flight. Calculated charge state distribution for different isotopes are shown in Figure 6. They were calculated with CHARGE code [70] for exit kinetic energy corresponding to magnetic rigidity $B\rho = 6.5$ Tm.

For the spatial separation of mono-isotopic beams in addition to the electromagnetic analysis an independent selection criterion is required. At high energy (30-2000 MeV/u) energy-degrader systems are used for this purpose, since the atomic energy loss (ΔE) of the ions penetrating through matter depends on Z^2. In this way the magnetic rigidity ($B\rho$) analysis is performed before and after the degrader. This is the so-called $B\rho - \Delta E - B\rho$ separation method [28].

A clear advantage of the in-flight separation is the short flight-time between the production target and the exit of the separator. This time is in the microsecond region and below and thus allows to study the most exotic nuclei.

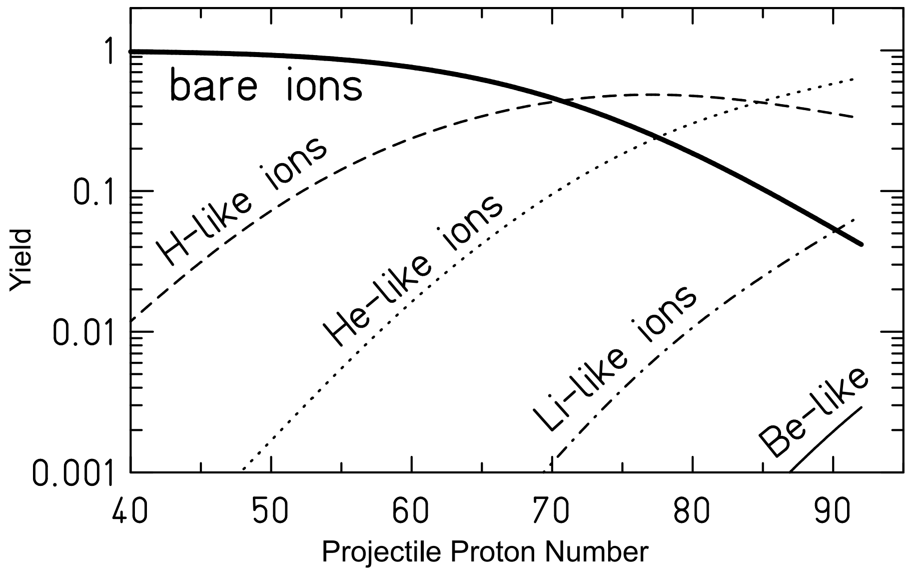

Fig. 6: Calculated with CHARGE code ionic charge state distributions for ions emerging from the production beryllium target with velocities corresponding to a fixed magnetic rigidity of 6.5 Tm. Taken from Ref. [61]

The separation in-flight depends mainly on kinematical properties, therefore, all nuclides can be provided without any chemical restriction. The disadvantage is that the nuclear reactions lead to inevitable phase-space enlargement of the separated beams, which can be compensated by coupling the in-flight facility to storage and cooler rings [29].

In-flight facilities based on projectile fragmentation are successfully used worldwide, e.g. at GANIL, GSI, JINR, MSU and RIKEN.

Both, the ISOL and in-flight, separation methods are highly complementary. The in-flight technique provides fast, clean and chemistry independent separation, the ISOL-technique is superior in terms of beam intensity for a number of elements and in terms of phase-space density. Presently, a hybrid technique is developed, whereby the fragments separated in-flight are thermalized in a gas cell [60]. Fast and efficient extraction out of the gas cell is then required before the rare-isotope beams of ISOL-quality are post-accelerated.

3 Storage ring facilities[2]

To efficiently use the rarely produced exotic nuclides, it is of a straightforward advantage to store them in a trapping facility. There are presently three laboratories where a combination of a radioactive-ion-beam with a storage-ring facilities is realised. Ion storage rings offer unique experimental conditions for precision experiments with stable and–if coupled to radioactive beam facilities–also with exotic nuclei. The research potential is enormous which was demonstrated in the last years by a number of successful experiments [43].

The facility at GSI Helmholtzzentrum für Schwerionenforschung was chronologically the first one to be taken into operation in 1990. The facility is schematically illustrated in Figure 7. It comprises the heavy-ion synchrotron, SIS, [7] the projectile fragment separator, FRS, [2, 28] and the experimental storage ring, ESR, [25]. A low-energy storage ring, CRYRING, which was until recently in operation at Stockholm university, is being presently installed behind the ESR [42], thus realizing the option (e) in Figure 1.

Intense beams of any stable isotope from protons up to uranium can be accelerated by the SIS to a maximum magnetic rigidity of $B\rho = mv\gamma/q =$ 18 Tm, where B is the applied magnetic field, ρ, m/q and v are the bending radius, the mass-over-charge ratio and the velocity of the accelerated particles, respectively, while γ is the relativistic Lorentz factor. Relativistic fragments with energies of several hundreds of MeV/u are produced mainly through fragmentation of primary beam projectiles in thick production targets. In the case of uranium primary beams also projectile fission is used for the production of neutron-rich nuclei. Typically beryllium targets with thicknesses of $1-8$ g/cm^2 are employed. Secondary beams are separated in flight in the FRS within about 150 ns and are then injected into the ESR. The maximal magnetic rigidity of the ESR is 10 Tm. Dependent on the specific experimental requirements, cocktail or clean mono-isotopic beams can be prepared with the FRS by employing magnetic rigidity ($B\rho$) analysis and atomic energy loss (ΔE) in specially shaped solid state degraders. Cocktail beams are ideally suited for the in-ring mass measurements [26], whereas pure mono-isotopic beams are often needed for lifetime determination or reaction studies [43]. The only significant disadvantage of the FRS-ESR facility is the low injection efficiency into the ESR, which is of the order of a few percents [61]. Exotic nuclei can also be produced in the direct

[2] Material for this section is taken from Refs. [47, 13, 43, 100]

transfer line connecting SIS and ESR by installing a production target in the stripper-foil station [15].

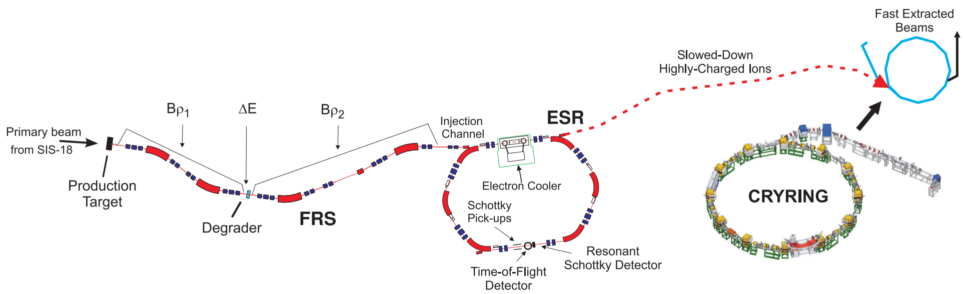

Fig. 7: The FRS-ESR arrangement at GSI. The two stages for in-flight $B\rho - \Delta E - B\rho$ separation and the energy degrader in the FRS as well as the electron cooler and the main detection systems in the ESR are shown. The foreseen location of the low-energy storage ring CRYRING (see insert) is indicated together with the beam-line connecting it to the ESR for transporting slowed-down highly-charged stable or radioactive ions. Taken from Ref. [86].

A similar scheme is realised at the Institute of Modern Physics, Chinese Academy of Sciences in Lanzhou, where a radioactive-ion beam facility is operated since 2007 [91, 93]. It is illustrated in Figure 8 and comprises the main cooler-storage ring, CSRm, used as a synchrotron, radioactive ion beam line in Lanzhou 2, RIBLL2, used as a fragment separator, and the experimental cooler-storage ring, CSRe. A detailed description of the HIRFL-CSR acceleration complex can be found in Refs. [91, 92, 99, 97]. As in the case of SIS-FRS-ESR, the primary beams extracted from the CSRm are fragmented in a beryllium (typically 1.5 cm in thickness) production target in front of RIBLL2, separated in flight and are injected into the CSRe. The CSRe has a mean circumference of 128.8 m and a maximal magnetic rigidity of 8.4 Tm. An advantageous difference of the CSRe in comparison to the ESR is that it has two longer straight sections which allow for more flexibility in designing reaction experiments and provide more space for detector setups. Several experiments are being considered in the CSRe which will profit from these properties.

The last but not least, the third facility, the Rare RI Ring (R3), was commissioned in 2015 at RIKEN Nishina Center in Japan [58]. Different from GSI and IMP complexes, the driver accelerator in RIKEN is not a syn-

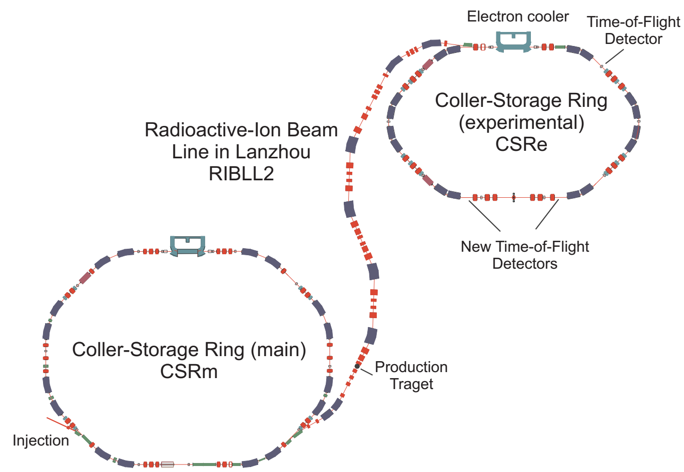

Fig. 8: Schematic layout of the high-energy part of the Cooler Storage Ring at the Heavy Ion Research Facility in Lanzhou (HIRFL-CSR) located at the Institute of Modern Physics in Lanzhou (IMP), Chinese Academy of Sciences. The heavy ion synchrotron CSRm, the in-flight fragment separator RIBLL2 and the experimental storage ring CSRe are indicated. Taken from [100]
. Courtesy to Yuhu Zhang.

chrotron but a superconducting ring cyclotron, SRC, which provides instead of a pulsed beam a quasi-DC beam. The facility is illustrated in Figure 9. It is important to stress that the highest beam intensities worldwide of, e.g., ^{238}U stable ions, are available at RIKEN.

After the separation, selected exotic ions can be injected into the corresponding storage ring. Heavy-ion storage rings are complicated facilities which can contain numerous components, like, e.g., kicker magnets to inject and extract particles, dipole magnets to bend the trajectories, quadrupole magnets to focus the particles, sextupole magnets to correct for aberrations, cooling devices, de-/acceleration cavities, various detector and diagnostic setups, etc. We note that the R3 ring is composed of only dipole magnets [84]. The arrangement of the ring magnets is called the "ring lattice".

In the rings precision experiments are successfully performed in nuclear structure and astrophysics (see, e.g, [102, 51, 90, 19, 83, 98], as well as atomic and fundamental physics (see, e.g., [14, 80, 50, 6, 56, 67, 36]). In cases of GSI and IMP facilities, the fast extraction of the primary beam from the synchrotron allows for storing all produced and transmitted to the ring

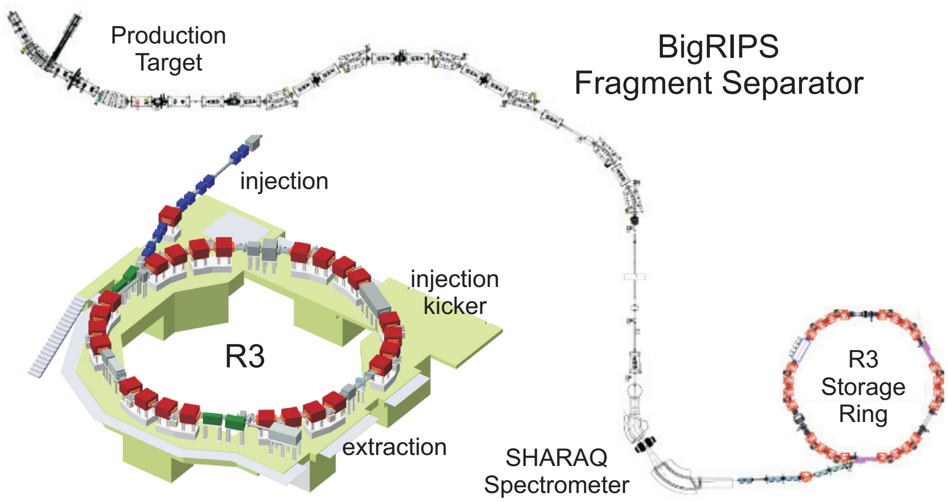

Fig. 9: Schematic view of the BigRIPS-R3 facility at RIKEN. Exotic nuclei produced in the production target are identified in flight with the BigRIPS separator. If an ion of interest is observed, the injection kicker is fired and the particle is stored in the R3 [58]. The inset shows a 3D model of the R3 ring. Taken from [100]
. Courtesy to Tomohiro Uesaka.

particles. In the case of the RIKEN setup, the DC-nature of the primary beam results in the storage and investigation of a single particle at a time. The biggest advantage of such system is that each particle is identified in BigRIPS [41] and no identification is needed in the storage ring itself.

Since the storage times in the ring can reach hours, different manipulations with the ions like beam cooling, slowing down, or preparation of clean mono-isomeric beams can be conducted (see, e.g., [69, 52, 15, 18]).

4 Basic equation of the storage ring spectroscopy[3]

Due to the Lorentz force, particles with different momenta are bent differently by the ring magnets and thus travel along different paths in the ring. Since the revolution time T is

$$T = \frac{L}{v}, \tag{1}$$

[3] Material for this section is taken from Refs. [26, 100]

where L, v are the path length and the velocity of the circulating particle. The fractional change of the revolution time or the revolution frequency $f = 1/T$ is

$$\frac{\Delta T}{T} = -\frac{\Delta f}{f} = \frac{\Delta L}{L} - \frac{\Delta v}{v}. \tag{2}$$

For particles that vary only in momentum, p, the velocity difference is:

$$\frac{\Delta v}{v} = \frac{1}{\gamma^2}\frac{\Delta p}{p}. \tag{3}$$

Here $\gamma = 1/\sqrt{1-\beta^2}$ is the relativistic Lorentz factor, $\beta = v/c$, and c speed of light in vacuum. Therefore, we can rewrite Eq. (2) as

$$\frac{\Delta T}{T} = \left(\alpha_p - \frac{1}{\gamma^2}\right)\frac{\Delta p}{p} = -\eta\frac{\Delta p}{p}, \tag{4}$$

where η and α_p are the so-called *phase-slip factor* and *momentum compaction factor*, respectively, connected as [26]

$$\eta = \frac{1}{\gamma^2} - \alpha_p = \frac{1}{\gamma^2} - \frac{1}{\gamma_t^2}, \tag{5}$$

where the *transition energy*, γ_t is defined as

$$\gamma_t \equiv \frac{1}{\sqrt{\alpha_p}}. \tag{6}$$

The physical meaning of α_p [26] is that it reflects the ratio between the relative change in the orbital length and the relative change in the magnetic rigidity $B\rho$ of the stored ions. The α_p can also be deduced from the dispersion function $D(s)$ of the ring.

$$\alpha_p \equiv \frac{dL/L}{d(B\rho)/(B\rho)} = \frac{1}{L_0}\oint \frac{D(s)}{\rho}ds. \tag{7}$$

Here s denotes the coordinate along the reference orbit L_0 in the ring, and ρ is the radius of the curvature of this reference orbit in the bending sections [26]. Detailed investigations of the α_p as a function of the ESR magnetic rigidity can be found in [95].

If a motion of particles with different mass-to-charge ratios, m/q, and momenta is considered, then the fractional momentum can be expressed as

$$\frac{\Delta p}{p} = \frac{\Delta(m/q)}{m/q} + \gamma^2\frac{\Delta v}{v}. \tag{8}$$

and Eq. (2) can be written as

$$\frac{\Delta f}{f} = -\frac{\Delta T}{T} = -\frac{1}{\gamma_t^2} \cdot \frac{\Delta(m/q)}{m/q} + \left(1 - \frac{\gamma^2}{\gamma_t^2}\right)\frac{\Delta v}{v}. \tag{9}$$

Equation (9) is the basic equation for storage ring mass spectrometry [62, 61]. In order to determine m/q values of the ions, one needs to measure their revolution frequencies or alternatively revolution times. The second term on the right hand side affects the achievable mass resolving power and for mass measurements it has to be made as small as possible. There are two ways to achieve the latter [26]. The first one is to reduce $\delta v/v$ by applying beam cooling.

5 Beam cooling[4]

The most important capability of storage rings is beam cooling, which allows the reduction of the energy spread of the stored ions induced, for instance, by the production reaction process, the interaction with internal targets, or due to recoiling in a decay.

Ion beams injected into a storage ring have intrinsic horizontal and vertical emittances, defined as product of beam size and angular divergence or of beam size and transverse momentum. At constant energy these emittances are fixed, due to Liouville's theorem, when applying conservative forces only. The action of focussing a beam, for instance, reduces its size, but at the expense of enlarged angular divergence (transverse momentum). The area of the phase-space ellipse "the emittance" always stays constant. The only way to reduce both size and momentum spread, i.e. to enhance the phase-space density, is to let the beam interact with non-Liouvillian devices, by using non-conservative forces. This is called "beam cooling". Three cooling techniques have been successfully applied until now to cool stored, fast ions: stochastic-, electron-, and laser-cooling. Laser cooling is the key to bring neutral atoms to rest and is used e.g. in magneto-otical traps. For highly charged ions it cannot be applied, except for a few cases of H-like or Li-like ions, where the condition of matching the electronic structure is fulfilled due to the hyperfine splitting of the ground state [89].

In contrast to laser cooling, stochastic as well as electron cooling are universal methods to cool all kinds of fast ions in both longitudinal and transverse directions. Stochastic cooling has been developed by van der Meer at CERN at the end of the seventies (Nobel Prize in Physics 1984).

[4] Material for this section is taken from Refs. [47, 13]

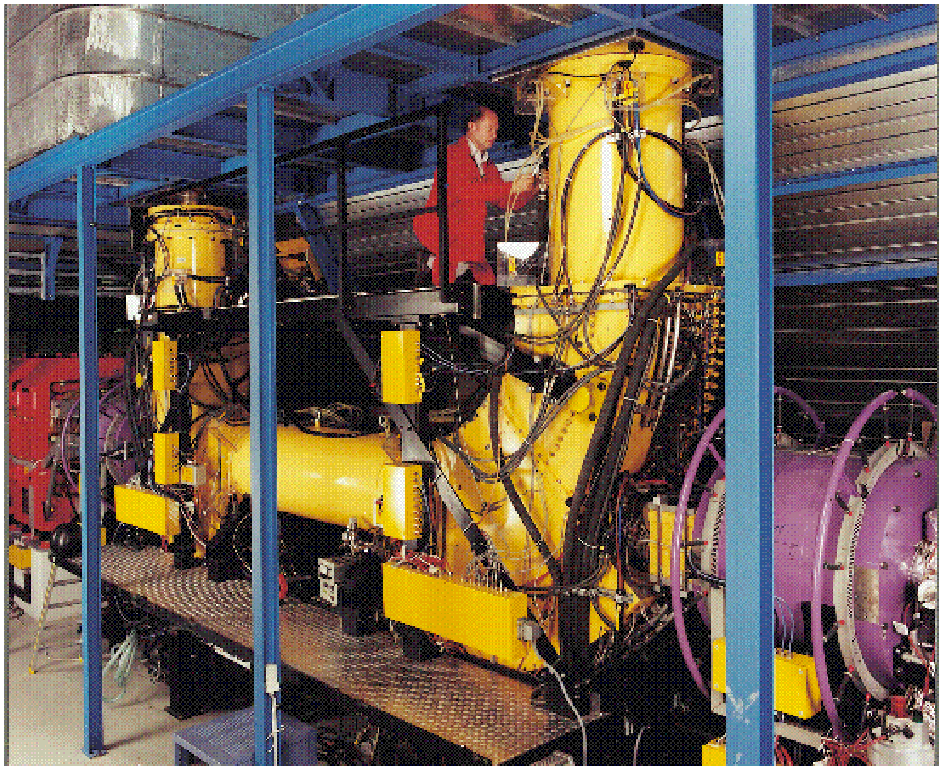

Fig. 10: Electron cooler at the ESR. The electrons have almost the same mean velocity as the ions but a much smaller velocity spread. The ion beam comes from bottom right, the electrons from top right, smoothly guided to and extracted from the common interaction zone (length about two meters) by a toroidal magnetic field. The ions come back after one turn of about 500 ns duration to interact again with fresh electrons. Along this region a longitudinal magnetic field of typically 0.05 T confines the electrons. Taken from Ref. [47]. Photo A. Zschau, GSI, Darmstadt.

Stochastic cooling is a kind of “self-correction” of the ion beam. A couple of plates (pick-up electrodes) registers deviations of the ions from the reference orbit as a difference of the signals induced onto the right and left plate, respectively. The signals are used to correct the ion motion within the same turn. Though the correction signal is appropriate for some ions but wrong for other ones, it can be shown that within a short time (typically 1 s for heavy ions) the average phase-space volume of the ion ensemble will be significantly reduced. Since stochastic cooling is most effective for "hot" beams ($\Delta p/p \geq 10^{-3}..10^{-2}$) it may serve as an ideal tool for pre-cooling, followed by electron cooling which is much less suited for this regime of large momentum spreads. For more details please see [54].

Electron cooling has been invented in the sixties of the last century by Budker in Novosibirsk and first realized there. To date it is the most widely applied cooling scheme, installed at almost all ion storage rings. It relies upon momentum exchange by Coulomb collisions between hot ions and collinear, cold electrons that are radially confined by a magnetic field of typically 0.01...0.1 T. After one interaction cycle (ions and electrons move in parallel for about a few meters) the electrons are extracted by a weak toroidal magnetic field, whereas the "old" ions come back after their next turn to interact with fresh, cold electrons, see Figure 10. The thermal equilibrium is reached within a short time, leading to an assimilation of both the longitudinal and transverse temperatures of electrons and ions. The cooling time is proportional to the cube of velocity spread of ions and inversely proportional to the square of atomic charge Z. Therefore, electron cooling is fastest for very heavy ions and small velocity spreads. For electron cooled beams, the momentum spread of stored ions $\delta p/p$ is determined by the equilibrium between the Coulomb interactions with cold electrons in the cooler device and the intra-beam scattering. The latter increases rapidly with increasing beam intensity and the atomic charge state of the ions. A momentum spread of $\delta p/p \sim 10^{-5}$ is achievable for 10^7 fully-ionised $^{238}U^{92+}$ ions, which is reduced by an order of magnitude for a few 10^3 stored ions. At even smaller numbers of stored ions a "phase transition" occurs, at which the intra-beam scattering is "switched off" and so-called "crystalline beams" with $\delta p/p$ of a few 10^{-7} are observed [73].

For a large initial velocity spread, the electron cooling can take up to a few minutes. However, if the stochastic pre-cooling, which is capable of reducing the momentum spread quickly to $\delta p/p \sim 10^{-4}$, is applied prior to the electron cooling, then the overall cooling time can be reduced to a few seconds [30]. Thus, cooled beams of radioactive ions with half-lives in the order of one second or longer can be prepared.

Stochastic and electron cooling techniques are applied in the ESR and CSRe which enable beams with the highest phase-space density. R3 does not employ any cooling and the precision experiments are based on a different technique.

6 Precision measurements of nuclear masses[5]

6.1 A short motivation

Three types of fundamental interactions, namely strong, weak, and electromagnetic, play–by acting between the nucleons–a major role in atomic nuclei. The sum effect of these interactions is reflected in the binding energy of the nucleus ($B(N, Z)$), which is directly connected with its mass ($m(N, Z)$) via a simple relation

$$m(N, Z) = N \cdot m_n + Z \cdot m_p - B(N, Z), \tag{10}$$

where N is the neutron number, Z is the proton number, m_n is the rest mass of the neutron, and m_p is the rest mass of the proton. Experimental nuclear masses are often used as a tool to reveal new nuclear structure effects [9]. Indeed, the shell structure and pairing correlations have been discovered via nuclear masses [9]. Accurate mass values are required for tests of the weak interaction, quantum-electrodynamics, and the Standard Model [8]. The actual pathways of the nucleosynthesis in stars are governed by the nuclear binding energies and lifetimes.

The birth of mass spectrometry can be associated with the first experiments of J. J. Thomson. In 1912 he has discovered the isotopic nature of the chemical elements [81]. Presently, after a century of measurements, the masses of about 2200 nuclides are known experimentally, as listed in the recent Atomic-Mass Evaluation AME'2012 [4].

Today, the challenge is to measure the masses and lifetimes of exotic nuclei close to the borders of their existence, driplines. These nuclides are usually called "exotic" or "rare" isotopes. They can reveal new nuclear properties due to the strong asymmetry of their proton-to-neutron ratio. However, they are difficult to investigate due to their small production cross-sections and short lifetimes. Therefore, very efficient and fast experimental techniques are required.

One of the important motivations for measuring atomic masses is the testing and further development of nuclear theories. The modern theories describe the known masses "quite" well but the predictions in unknown territories diverge [72], see Figure 11. A big part of neutron-rich nuclei is unaccessible presently at the modern radioactive beam facilities, and their properties have to be determined theoretically.

The required mass accuracy varies for different applications. Some examples are listed in Table 1. The most accurate measurements are done

[5] Material for this section is taken from Refs. [26, 12, 43, 100]

nowadays employing ion traps [8].

Tab. 1: Several examples for mass measurements with typical required relative mass accuracy $\delta m/m$ [8].

Application	Required mass accuracy $\delta m/m$
Molecular mass spectrometry	$10^{-4} - 10^{-6}$
Nuclear shell structure	$10^{-6} - 10^{-7}$
Nuclear mean-field models	10^{-6}
Nucleosynthesis processes	10^{-7}
Atomic binding energies	$10^{-9} - 10^{-10}$
Metrology, fundamental symmetries	$10^{-10} - 10^{-11}$

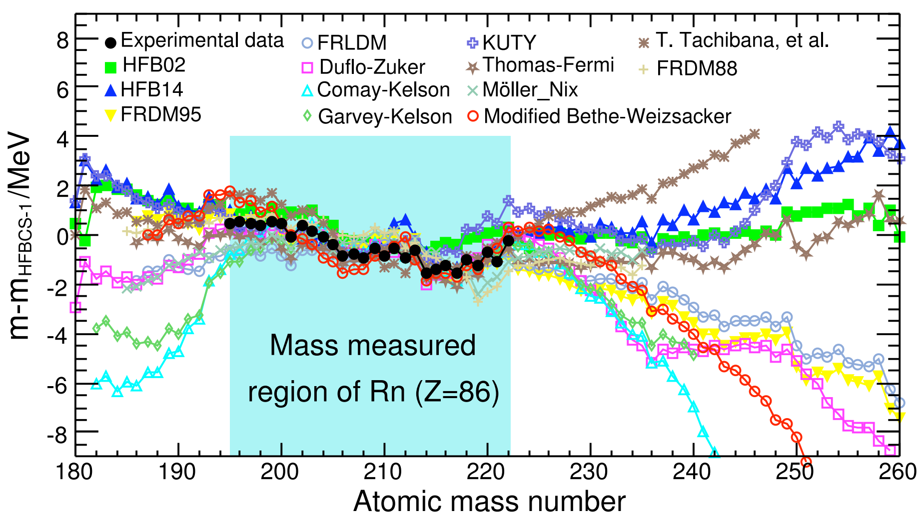

Fig. 11: Comparison of different mass models and experimental data for Rn isotopes. The models describe rather well the known masses but diverge quickly in yet unknown regions. Courtesy to Lixin Chen.

6.2 In-ring Mass Spectrometry

Two complementary experimental methods, namely Isochronous (IMS) and Schottky (SMS) Mass Spectrometry, have been proposed for accurate mass measurements, see Figure 12.

In the SMS, the velocity spread can be reduced by stochastic and electron cooling, which force all stored ions towards the same mean velocity and thereby reduce the velocity spread to roughly $5 \cdot 10^{-7}$ for beam intensities

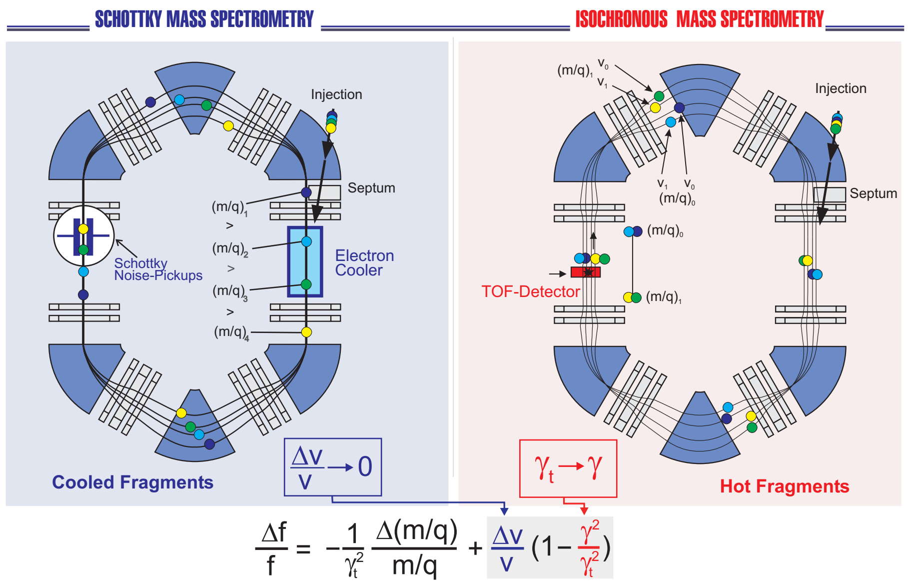

Fig. 12: The two kinds of mass spectrometry applied at a ring by measuring the revolution frequencies of stored exotic ions. Left hand side: Schottky mass spectrometry. Here the ions are electron-cooled, therefore their velocity spread Δv gets negligibly small. Their revolution frequencies are measured by pick up plates mounted in the ring aperture. This technique has been successfully applied at longer-lived exotic nuclei. Right hand side: Isochronous mass-spectrometry. Uncooled ions circulate at the transition energy γ_t. Their revolution times are measured by a time-of-flight technique. This method is in particular suited for short-lived nuclei with half-lives in the millisecond- or even microsecond range. Courtesy to Torsten Radon.

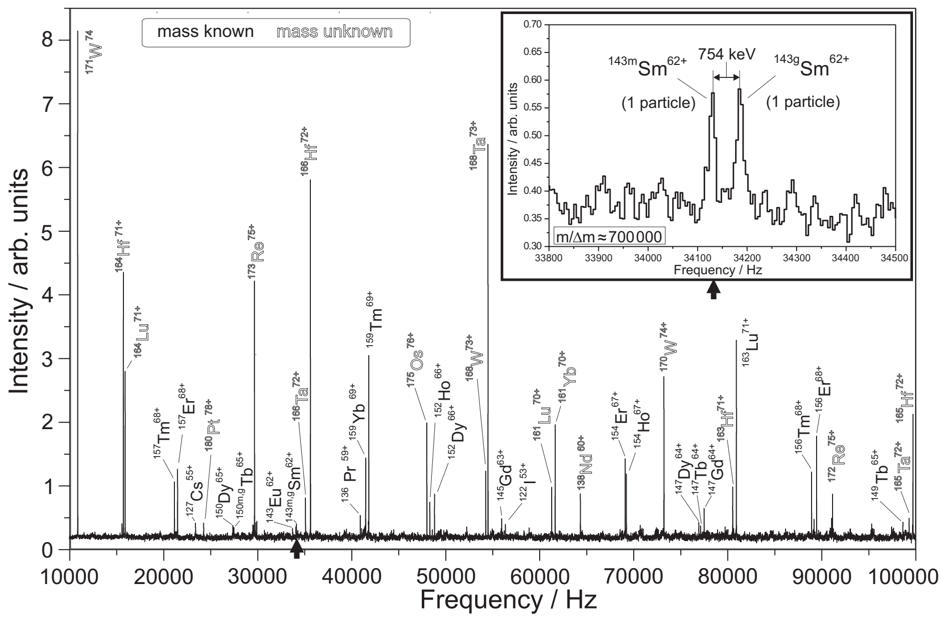

Fig. 13: Schottky spectrum of fragments from a primary ^{209}Bi beam, stored and electron-cooled in the ESR. The measured frequency bandwidth is 320 kHz which cover the full acceptance of the ESR. The shown here spectrum covers about 1/3 of the whole measured range. The inset shows a zoom into the spectrum with the well-resolved ground and isomeric state of bare $^{143}Sm^{62+}$, each of them populated by one single ion. Taken from Ref. [13]

below about 2000 ions. Thus the second term in equation (9) becomes negligible and the measured revolution frequencies reflect directly the mass-to-charge ratios of the stored ions. The revolution frequencies are measured by the Schottky-noise spectroscopy.

Every ion, q-times charged, induces at each passage a signal proportional to q^2 onto a couple of plates mounted in the ring aperture (Schottky noise pick-ups). These signals are sampled, Fourier transformed and mixed with a local oscillator to convert the original revolution frequencies into a frequency range of a few hundred kHz. In principle, all harmonics of the fundamental revolution frequency (typically 2 MHz) can be used for this purpose. A data acquisition system records a large bandwidth, wide enough to cover the frequencies of all stored ions simultaneously, with a high resolution of a

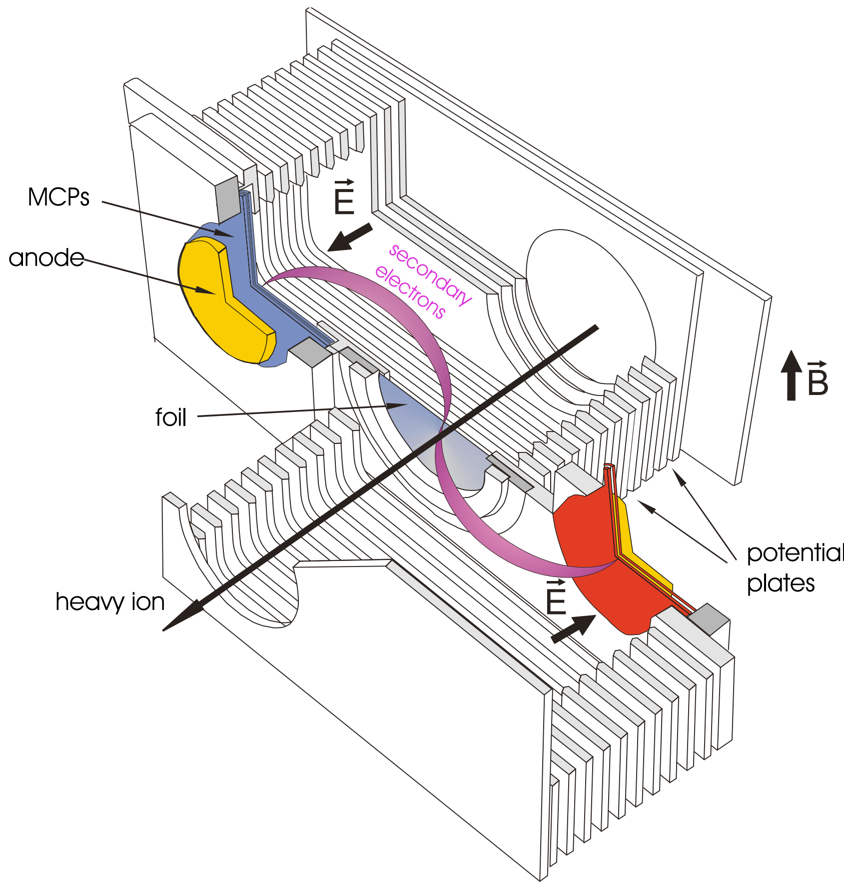

Fig. 14: Schematic layout of the time-of-flight detector. The ions penetrate a thin carbon foil and release secondary electrons. These are transported by crossed magnetic and electric fields onto the micro-channel-plate detectors. The detectors are directly connected to the fast sampling oscilloscopes and provide fast timing signals. Taken from Ref. [100]. Courtesy to Milan Matoš.

few Hz. An example of measured Schottky frequency spectrum is illustrated in Figure 13.

Schottky mass spectrometry shows very specific and partially unique features. This technique offers a presently unsurpassed effciency: many tens masses can be determined simultaneously, i.e. with one filling of the storage ring, provided that appropriate nuclei with known masses are measured in the same spectra for the purpose of calibration. The ultimate detection detection of one single stored ion is impressive. Although the mass resolving-power $m/\Delta m \approx 10^6$, corresponding to an accuracy of about 30 keV for heavy nuclei, cannot compete with world best measurements of 10^{10} accessible in ion traps, it is by far sufficient for a broad mass-mapping of exotic nuclei far from stability, see Table 1. For the time being, this opportunity to simultaneously perform a mass spectroscopy of isobars is unrivalled. The disadvantage of SMS is that the cooling process lasts a few seconds. Thus, only the nuclides with half-lives longer than about 1 second can be investigated.

Exotic nuclei with half-lives shorter than the cooling time can be investigated with a time-of-flight technique by operating the ring in the isochronous mode. In this case the ions of interest are injected into the ring with $\gamma = \gamma_t$. Thus, the term containing the velocity spread in equation (9) is (in first order) equal to zero, i.e. the revolution frequency of the circulating fragments does not depend on their velocity spread. A time-of-flight detector is used to measure the revolution frequencies. The detector is schematically shown in Figure 14 [82]. This detector records time stamps of each ion passing

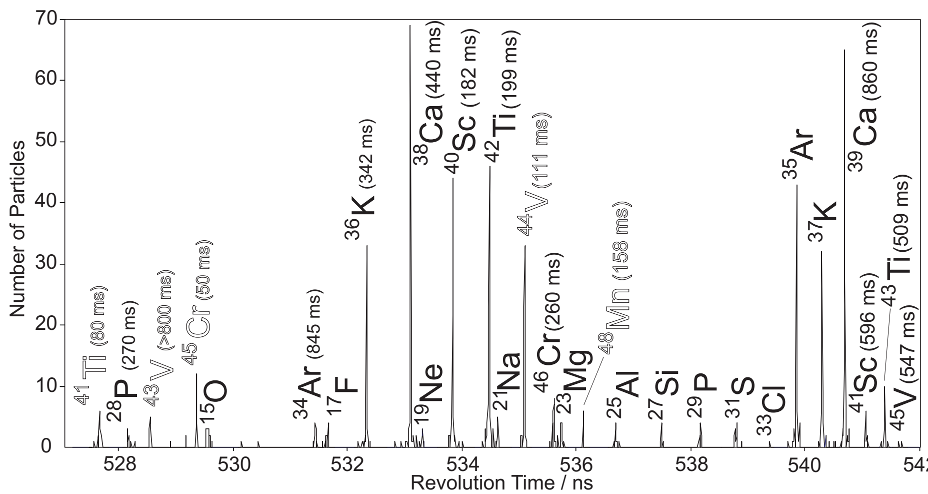

Fig. 15: Revolution time spectrum of fragments of a primary ^{52}Cr beam, taken by the TOF detector. Previously unknown masses are indicated by outlined letters. Taken from Ref. [30].

through it at each revolution. It is equipped with a very thin carbon foil (about 4-17 μg/cm^2). The ions penetrating the foil release secondary electrons on both sides of the foil. These electrons are guided by the electric and magnetic fields to the set of micro-channel plates which are used for fast timing signals. The time signals can be converted into the revolution frequencies of the stored ions. A typical measured time-of-flight spectrum is shown in Figure 15. The fragments do not require cooling and the nuclei with half-lives as short as 10 μs–about 20 revolutions in the ring–can be measured with this method. For instance, the nuclide with the shortest half-live measured by the IMS is the isomeric state observed in ^{133}Sb nuclide at an excitation energy of $E^* = 4.56(10)$ MeV [78, 77]. The half-life of this isomer in neutral atoms is $T_{1/2}^{\mathrm{atom}} = 16.54(19)$ μs [4]. However, due to the fact that bare ^{133}Sb nuclei were stored in the ring, all decay modes involving bound electrons were disabled [46] and a half-life in the order of 10 ms is expected [77].

In-ring mass measurements of exotic nuclei were pioneered in the 1990s at GSI [29], and are now conducted at both, ESR and CSRe storage rings. R3 was commissioned in 2015 and the first measurements of new masses are planned in 2016. To date all Schottky mass measurements were conducted solely in the ESR. Isochronous mass spectrometry is applied at all three storage ring facilities.

Storage ring mass spectrometry together with cocktail beams offered by the corresponding separators, enables broadband investigations of many tens of nuclear species in a single measured spectrum. For instance a single spectrum in the isochronous mode covers $\Delta(m/q)/(m/q) \approx 13\%$ [34]. A part of the revolution time spectrum of ^{58}Ni projectiles addressed by the IMS at CSRe [101, 96] is illustrated in the upper insert of Fig. 17. Many nuclei with previously unknown (roman) and known (italic) masses are simultaneously measured. The nuclides with known masses provide an *in situ* calibration of the revolution time / frequency spectra.

Storage ring mass spectrometry is an extremely sensitive technique. Often a single stored ion is sufficient to determine its mass with high accuracy. One example of such measurement is illustrated in Fig. 17, where a Schottky frequency spectrum of stored ^{238}U projectile fragments is shown in the lower insert [16]. The frequency peak at about 125 kHz corresponds to a single ^{208}Hg nucleus which was seen once as a H-like ion within a two-weeks long experiment. Furthermore, six new isotopes have been discovered in the ESR together with their mass and half-life measurements [17]. They are indicated with white asterisks on the chart of the nuclides in Figure 17.

The sensitivity of the SMS to single stored ions can be used to resolve low-lying isomeric states, which could otherwise not be resolved. Figure 16 illustrates the discovery of a long-lived isomeric state with an excitation energy of $E^* = 103(12)$ keV in the neutron-deficient ^{125}Ce nuclide [79]. Combined with the capability of storage rings to cover a wide range of different nuclides in one frequency spectrum, the single ion sensitivity can be used for a broadband search of nuclear isomers on the chart of the nuclides. For instance, a region of neutron-rich nuclei around ^{188}Hf is predicted to exhibit isomers with exceptional properties [85, 21]. It was recently mapped using SMS [71, 63, 65, 64].

The harvest of masses obtained for the first time via storage ring mass spectrometry is illustrated on the chart of the nuclides in Fig. 17 [100]. The achieved relative mass accuracy spans from a few 10^{-7} (SMS) to $10^{-6} - 5 \cdot 10^{-7}$ (IMS). The new masses enabled numerous investigations of nuclear structure and astrophysics questions which are not possible to cover within this review. For more details, the reader is referred to Refs. [13, 26, 11] and references cited therein.

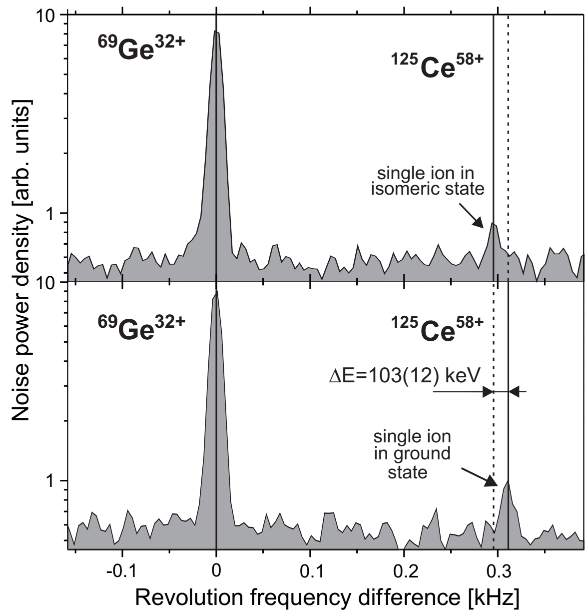

Fig. 16: Schottky frequency spectra of two measurements in the ESR of single stored fully-ionised $^{125}Ce^{58+}$ ions in the isomeric (upper panel) and ground (lower panel) states. The frequency peak of $^{69}Ge^{32+}$ ions can be used as a reference. The frequency difference between the two single ^{125}Ce ions corresponds to the isomeric excitation energy of $E^* = 103(12)$ keV. Taken from [79].

7 Lifetime spectroscopy in storage rings[6]

7.1 A short motivation

With the FRS-ESR, it became possible to produce unstable, highly-charged ions and to inject them into a storage ring [29]. Here, owing to the ultra-high vacuum of $10^{-10} - 10^{-12}$ mbar, the high atomic-charge states can be preserved and constantly monitored for extended periods of time sufficient to study decay properties of such highly-charged ions [47].

Interest in such investigations is manyfold: A straightforward example is that highly-charged ions enable one to study the influence of bound electrons on the radioactive decays. Here the bare or H-like heavy ions represent

[6] Material for this section is taken from Refs. [47, 13, 43]

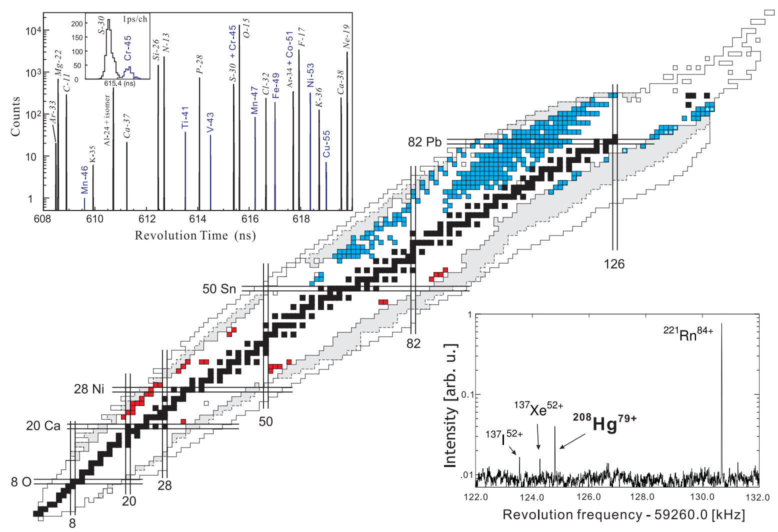

Fig. 17: The chart of the nuclides illustrating nuclides whose masses were measured by storage ring mass spectrometry at ESR and CSRe, and those which could be determined by using literature Q-values of proton and α-decays. Only the ground-state masses obtained for the first time are considered. The white area indicates the nuclides with known masses according to the atomic mass evaluation AME'12 [4]. The grey area with dashed-line borders indicates the range of nuclides which can be addressed by storage ring mass spectrometry at the present ESR and CSRe [94]. The outer white region with solid-line borders is the area of nuclides that will become accessible at the future FAIR facility; the goal of the ILIMA proposal [86]. The masses stemming from SMS and IMS are indicated by blue and red colours, respectively. The upper insert shows a part of the revolution time spectrum of ^{58}Ni projectile fragments measured by IMS in the CSRe. Taken from [101]. The lower insert illustrates a 10 kHz part of a Schottky frequency spectrum of neutron-rich ^{238}U projectile fragments. A single H-like $^{208}Hg^{79+}$ ion was seen only once in a two-weeks long experiment. Taken from Ref. [16].

well-defined quantum-mechanical systems in which the corrections due to otherwise many bound electrons are removed. Obvious examples are the decays of fully-ionised atoms in which the decays involving electrons are just disabled [46]. Furthermore, new decay modes–strongly suppressed or disabled in neutral atoms–can open up. Another motivation for such studies are the nucleosynthesis processes in stars, where the involved nuclides are usually highly-charged due to high temperatures and high densities of the corresponding environments. For instance in the s-process along the valley of β stability the mean "temperature" (kT) amounts to about 30 keV and in the explosive r-process it reaches more than 100 keV.

We focus here on the studies of weak decays. Using p, n, e^-, e^+ and ν_e to indicate the proton, neutron, electron, positron and electron neutrino, respectively, the latter can be summarised as:

$$p + e_b^- \rightarrow n + \nu_e \qquad \text{orbital electron capture (EC);} \tag{11}$$
$$p \rightarrow n + e^+ + \nu_e \qquad \text{continuum } \beta^+ \text{ decay } (\beta_\mathrm{c}^+); \tag{12}$$
$$n \rightarrow p + e^- + \bar{\nu}_e \qquad \text{continuum } \beta^- \text{ decay } (\beta_\mathrm{c}^-); \tag{13}$$
$$n + \nu_e \rightarrow p + e_b^- \qquad \text{bound} - \text{state } \beta - \text{decay } (\beta_\mathrm{b}^-). \tag{14}$$

In the decay the mass-over-charge ratio changes which inevitably leads to a change of the revolution frequency in the ring between parent and daughter ions. In the two-body β-decays (11) and (14), the charge state is not altered and the frequency change is small and directly reflects the decay Q-value. In the three-body decays (12) and (13) the charge is modified as well which results in a much bigger frequency change.

In case that the frequencies of both, the parent and the daughter ions lie within the storage acceptance of the ring, they can be addressed by the time-resolved SMS [45]. An example is illustrated in Fig. 18, where the daughter H-like $^{175}\mathrm{W}^{73+}$ ions are populated via EC and β_c^+ decays of respectively He-like $^{175}\mathrm{Re}^{73+}$ and H-like $^{175}\mathrm{Re}^{74+}$ parent ions.

Particle detectors inserted into the ring aperture after a dipole magnet can be employed to detect daughter ions if their orbits lie outside the ring acceptance. In such case, the beam of parent ions, the intensity of which is monitored by the SMS, circulates undisturbed on the central orbit of the ring and the created daughter ions are deflected by the magnet and are intercepted by the detector. In both cases a redundant measurement is achieved in which the decay curve of the parent ions and the growth curve of the daughter ions are simultaneously measured. A principle of the in-ring lifetime spectroscopy is illustrated in Figure 19.

7.2 Beta decay of highly-charged ions

Although half-life measurements can be done at all three storage ring facilities, to date all in-ring investigations of radioactive decays of highly charged ions were conducted at the ESR.

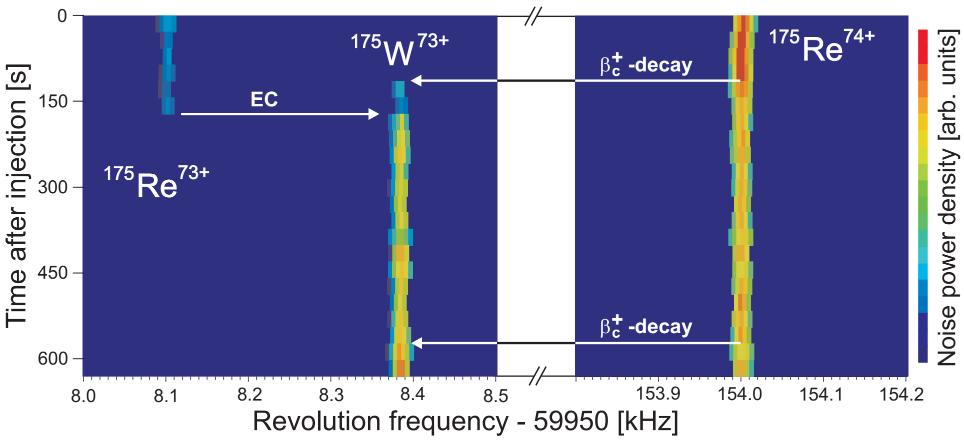

Fig. 18: Time-resolved Schottky frequency spectra of stored isobars with $A = 175$. Three H-like $^{175}\mathrm{W}^{73+}$ ions are created in radioactive decays in the ESR. One ion is produced in the EC decay of a single He-like (He-like) $^{175}\mathrm{Re}^{73+}$ ion at about 3 min after injection. The other two ions are created in three-body β_c^+-decay of two out of a few stored H-like $^{175}\mathrm{Re}^{74+}$ ions at about 2 and 10 min after the injection. Taken from [47].

Several exciting experimental results have been obtained. The bound-state β_b^- decay was experimentally discovered in fully-ionised ^{163}Dy atoms. Neutral ^{163}Dy are stable but decay with $T_{1/2} = 33$ days if stripped off all bound electrons [35]. This measurement led to a determination of the temperature in the s-process and set an upper limit for the mass of the electron neutrino. Another example is the β_b^- decay of $^{187}\mathrm{Re}^{75+}$ nuclei [10]. Neutral ^{187}Re atoms decay with $T_{1/2} = 42 \cdot 10^9$ years to ^{187}Os atoms. The decay energy $Q_{\beta_c^-} = 2.7$ keV is the smallest known $Q_{\beta_c^-}$ value [4]. However, the bare ^{187}Re nuclei decay by merely $T_{1/2}(^{187}\mathrm{Re}^{75+}) = 33(2)$ years, which is by more than 9 orders of magnitude shorter than the half-life of neutral atoms. Being a pure r-process nucleus ^{187}Re shields ^{187}Os, which can thus not be produced in the r-process. Therefore, owing to the long half-life of ^{187}Re, it was suggested to use the ^{187}Re/ ^{187}Os pair as a cosmic clock to determine the age of the Universe. Since ^{187}Re can be present in different charge states during the galactic evolution, the much faster β_b^--decay has to be taken into account.

In recent experiments, β_b^-/β_c^- ratios could be measured for the first time in neutron-rich nuclei. Such ratios are analogous to the EC/β_c^+ ratios mea-

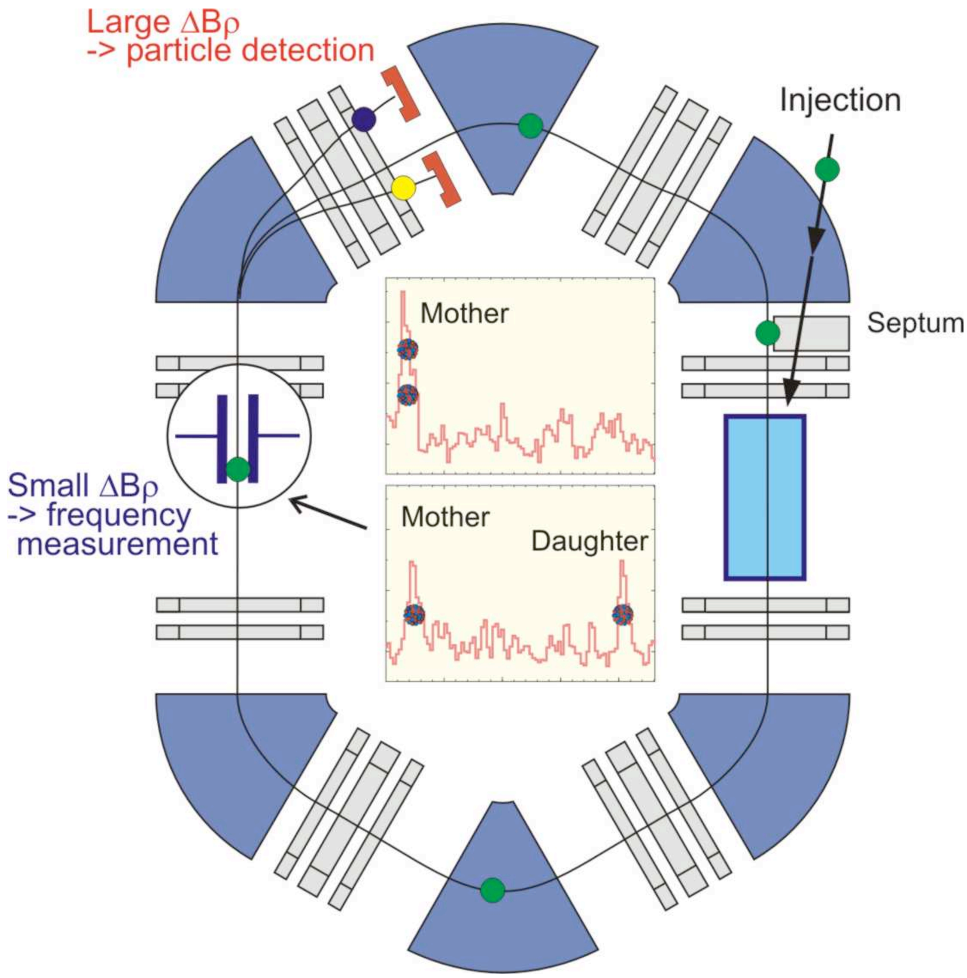

Fig. 19: Principle of life-time spectroscopy in storage rings. The intensities of stored ions can be monitored applying time-resolved SMS. In this method redundant information can be obtained, namely the decay of the parent ions can be measured simultaneously with the growth of the daughter ions. The second approach is to employ particle detectors behind bending magnets. Since the mass and often also the charge is changed in the radioactive decay, the daughter ions have different bending radii and can be intercepted with such detectors. Courtesy to Hans Geissel.

sured on the neutron-deficient side and can be used to test the β-decay theory. Decays of bare $^{206}Tl^{81+}$, $^{207}Tl^{81+}$ [57] and $^{205}Hg^{80+}$ have been studied. Except for a slight deviation in the latter case, the decay rates can well be described by using standard β-decay calculations.

Measurements of allowed $1^+ \to 0^+$ Gamow-Teller EC-decay of H- and He-like ^{140}Pr and ^{142}Pm ions yielded a striking result [48, 88]. The EC-decay rates in H-like ions turned out to be about 50% larger than in the corresponding He-like ions, though the number of the bound electrons is reduced from two to one. This counterintuitive effect could be explained if the total angular momentum of nucleus plus lepton system is considered [59]. Dependent on the spin-parities of the parent and daughter nuclei as well as on the magnetic moment of the former, the allowed EC-decay can be disabled in H-like ions though a bound electron is present. The first attempt to confirm this was done by studying the decay of highly-charged ^{122}I ions [3].

Another, yet unexplained but broadly discussed in literature, effect of the EC-decay studies of H-like ^{140}Pr and ^{142}Pm ions in the ESR is the observed 7 s modulation superimposed on the exponential decay curve [44].

8 Reactions with stored exotic ions[7]

For in-ring reaction experiments internal targets can be used. Normally gas or cluster targets are employed. A wide range of gases like H_2, d, ^{3}He, ^{4}He, Ar, Xe, CH_4, etc. can be utilised. The targets have small dimensions of less than 10 mm at the interaction zone and are very thin having thicknesses of $< 10^{15}$ atoms/cm^2. This enables a very high angular and energy resolution in reaction measurements and access to measurements at very low momentum transfer where low energy recoil particles need to be detected. Furthermore, such targets are windowless, which is essential since no corrections are needed to subtract the background from the interactions in windows. Although the targets are thin, relatively high luminosities are obtained owing to high revolution frequencies of the ions in a ring, which are typically $10^5 - 10^6$ Hz. Assuming a stored beam with a moderate intensity of 10^5 ions, a luminosity of $10^{25} - 10^{26}$ /cm^2·s can be achieved. We note that densities in excess of 10^{14} atoms/cm^2 can be achieved by using droplet targets, which, however, affects the excellent properties of the cooled beams.

First in-ring nuclear reaction studies were conducted in the last few years in the ESR. The first experiments are planned in the CSRe.

The first example is the proton capture reaction measurement relevant

[7] Material for this section is taken from Ref. [43]

for the p-process of nucleosynthesis. The favoured sites for the p-process are the explosively burning O / Ne layers in the type-II Supernovae and the explosive carbon burning in the type-Ia Supernovae, which last for about 1 s and can be characterised by high temperatures of $2-3\cdot10^9$ K and densities of about 10^6 g/cm^3 [see script of R. Reifarth from 2014] . The astrophysical p-process involves about 2000 nuclei connected by more than 20000 reactions, mainly (γ,n), (γ,p) or (γ,α). However, only a handful of experimental data for stable isotopes has been determined in the Gamow window of the p-process so far.

Storage rings offer the possibility to address capture reactions on unstable ion beams. The proof-of-principle experiment addressing a proton capture reaction relevant for the astrophysical p-process was performed in 2009 [102]. A primary beam of $^{96}_{44}$Ru projectiles was fully-striped of electrons in an 11 mg/cm^2 carbon foil placed in the SIS-ESR transfer line. The fully-ionised atoms were injected at 100 MeV/u, stored, electron cooled and decelerated to 9, 10 or 11 MeV/u. About $5\cdot10^6$ ^{96}Ru^{44+} ions were stored and cooled at the final energy. Taking into account the revolution frequency of about 500 kHz and the thickness of the H_2 target of about 10^{13} atoms/cm^2, a luminosity of about $2.5\cdot10^{25}$ /cm^2·s is achieved. The main reaction channel in the target is the atomic electron pick-up (REC) from the target atoms which is accompanied by an emission of an X-ray. Moreover, the charge state of ^{96}Ru ions is changed from 44+ to 43+ and the ^{96}Ru^{43+} ions can be detected by particle detectors inside the first dipole magnet downstream of the gas-jet target. Since the K-shell REC cross sections are known to about 5%, the X-rays detected in coincidence with ^{96}Ru^{43+} ions provide an *in situ* measurement of the luminosity. The nuclear reaction products of (p,γ), (p,n) and (p,α) reactions, the ^{97}Rh^{45+}, ^{96}Rh^{45+} and ^{93}Tc^{43+} ions, respectively, are bent to inside orbits by the dipole magnet and are detected by position sensitive double-sided silicon strip detectors (DSSD). The DSSDs are installed in air in vacuum pockets separated from the ring vacuum by 25 μm stainless steel windows. The measured ^{96}Ru$(p,\gamma)^{95}$Rh cross-section at 10 MeV/u was determined to be 3.6(5) mbar [51].

Unfortunately, the daughter ions with energies of below 10 MeV/u were stopped in the vacuum window and the gas in front of the DSSD, which did not allow the measurements directly in the Gamow window of the p-process. Further investigations of (p,γ) as well as (α,γ) reactions are proposed for the ESR as well as for the CSRe [90].

The second example addresses the physics of X-ray bursters. Astrophysical X-ray bursts have been interpreted as being generated by thermonuclear explosions in the atmosphere of an accreting neutron star in a close binary system [87]. In between the bursts, energy is generated at a constant rate by the hot CNO cycle driven by the in-flow of hydrogen and helium material from the less evolved companion star. The $^{15}O(\alpha,\gamma)^{19}Ne$ reaction is a probable candidate for a breakout reaction from the CNO cycle, which then fuels the *rp*-process. The latter can result in the production of neutron-deficient nuclei, possibly up to Sn-Sb elements [68]. The $^{15}O(\alpha,\gamma)^{19}Ne$ reaction rate controls the conditions for the ignition of the X-ray burst. This is a resonant reaction, in which the key resonance is at $E_r = 504$ keV, corresponding to a $3/2^+$ state at an excitation energy of 4.033 MeV in ^{19}Ne. This state decays predominantly by γ-decay, and a very weak α-decay branch of about 10^{-4} was predicted to exist. The latter is the key quantity which determines the resonance strength and which has to be verified experimentally.

Now, a proof of principle experiment has been proposed and conducted in the ESR in October 2012 addressing the population of the key 4.033 MeV state in ^{19}Ne via the (p, d) reaction on stable ^{20}Ne nuclei [19]. Fully-ionised $^{20}Ne^{10+}$ atoms were stored and cooled in the ESR at 50 MeV/u. A hydrogen gas-jet target with a density of 10^{13} atoms/cm^2 has been employed. A DSSD detector was inserted on the inner side of the ESR 50 cm downstream the interaction point. This detector was used to measure the energies of the emitted deuterons. A good energy resolution could be achieved online. The decay products of the $^{19}Ne^*$ ions, $^{19}Ne^{10+}$ or $^{15}O^{8+}$ ions, after α-decay, were detected with a PIN-diode detector mounted on the outside of the ESR about 8 m downstream the interaction point.

In an ideal case, for each detected deuteron corresponding to the populated 4.033 MeV state in $^{19}Ne^*$, a $^{19}Ne^{10+}$ or $^{15}O^{8+}$ ion shall be detected in coincidence. We note that this is the first transfer reaction ever measured in the ESR. The data analysis is in progress.

Another example concerns the light-ion induced direct reactions, which are planned within the so-called EXL project [38]. Such reactions, like for example elastic and inelastic scattering, transfer, charge-exchange, or knockout reactions, have been shown in the past, for the case of stable nuclei, to be powerful tools for obtaining nuclear structure information. In the last two decades they have also been used for the investigation of exotic nuclei with radioactive beams in inverse kinematics. In particular, it turned out that in many cases essential nuclear structure information is deduced from high-resolution measurements at low momentum transfer. For the case of inverse kinematics experiments with radioactive beams, such measurements can be favourably performed with radioactive beams, stored and cooled in storage rings, and interacting with thin internal gas-jet targets. This technique enables, due to the thin windowless targets and the beam cooling, to perform high resolution measurements, even for very slow target-like recoil particles, obtained from reactions at low momentum transfer with reasonable luminosity by profiting from the accumulation and recirculation of the radioactive beams.

A pioneering proof-of-principle experiments started recently at the ESR employing stable ^{58}Ni and radioactive ^{56}Ni beams [98]. Interactions of these beams with internal hydrogen and helium gas-jet targets were used to study the experimental conditions for reaction experiments in the environment of a storage ring. The angular distribution for elastic proton scattering from the doubly-magic ^{56}Ni was measured in order to obtain a deeper insight into the structure of this nucleus, which is of high interest from the nuclear structure and nuclear astrophysics points of view. It should be pointed out that this experiment was, even on a world-wide scale, the first of this kind performed with a radioactive beam [38].

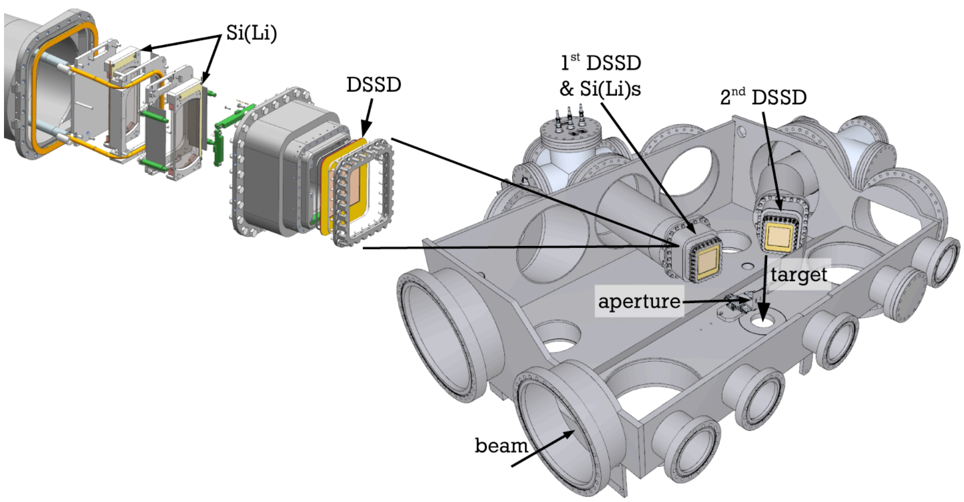

Fig. 20: Schematic view of the EXL setup recently used for reaction experiments at the ESR [38]. For details see text. Courtesy to Peter Egelhof.

Within the last years a dedicated innovative experimental setup was designed and constructed for these experiments on the basis of the results obtained within the R&D investigations for the EXL project [83]. The setup (see Fig. 20) consists of a UHV-compatible detector chamber which allows for installing, besides the internal gas jet target, UHV-compatible detectors for target-like reaction products in a relatively large angular range, as well as the necessary infrastructure for performing direct reaction experiments.

A ^{56}Ni beam with an intensity of about $7 \cdot 10^4$ particles per spill was produced by fragmentation of ^{58}Ni projectiles in the FRS and then injected at an energy of 400 MeV/u into the ESR. After stochastic cooling, bunching and stacking a stored and cooled beam of about $5 \cdot 10^6$ ^{56}Ni ions was available, which resulted–taking into account the density of the H_2 target of about $2 \cdot 10^{13}$ atoms/cm^2–in a luminosity of about $2 \cdot 10^{26}$ /cm$^2\cdot$s. The data analysis is in progress. Preliminary results on the elastic and inelastic proton scattering from ^{56}Ni can be found in [98].

9 Future Storage Ring Facilities[1]

9.1 Storage ring at HIE-ISOLDE

Recently a project has been initiated to couple a storage ring to the HIE-ISOLDE facility (see Figure 5) at CERN [33]. An important distinctive feature of this project is that the ion beams will be produced by the Isotope Separation On-Line (ISOL) method, whereas all existing storage ring facilities are based on the in-flight production of secondary beams at high energies. Thus the option (d) in Figure 1 will be realized for the first time. This offers advantages in terms of the beam intensity for a large number of elements and the beam quality. Moreover, the existing and planned post-acceleration schemes can deliver high-quality ISOL beams right at the required energies, which circumvents the long slowing down times required for the relativistic ion beams.

The Test Storage Ring (TSR), which operation was stopped at the Max-Planck Institute for Nuclear Physics in Heidelberg in 2012, is perfectly suited for this purpose. The physics scope of this instrument includes nuclear physics, nuclear astrophysics and atomic physics, with several experiments that can only be done there. Examples of the proposed experiments include the measurement of the half-life of ^{7}Be in a H-like state, which is of importance for the models of the Sun, nuclear structure studies far from stability through nuclear reactions and decay of ions circulating in the ring, research on nuclear isomers, etc. Also suggested are investigations on nuclear ground-state properties of exotic nuclei via the hyperfine effects on the atomic levels, which can be probed with an unprecedented resolution using dielectronic recombination. The physics motivations are elaborated in detail within an extensive Technical Design Report published recently [33].

[1] The text adopted from Ref. [43]

9.2 CRYRING at ESR

The Stockholm CRYRING is an immensely successful ion storage ring, which has enabled seminal research contributions in atomic and molecular physics for many years. As part of the Swedish contribution to FAIR, the CRYRING was transported to GSI. It is planned to reassemble the CRYRING in the coming two years (see Fig. 7). With the combination of the ESR and the CRYRING a unique facility – depicted as option (e) in Figure 1 – will be created, which provides cooled, highly-charged ion beams at low energies. Thus stored and cooled highly-charged ions up to fully-ionised uranium will be available at GSI in the wide energy range from about 400 MeV/u down to 4 MeV/u in the ESR and then down to a few tens of keV/u in the CRYRING. Moreover, the CRYRING can operate independently with its own ion source. Thus, CRYRING is excellently suited as a test bench for FAIR for testing technologies and instruments developed for FAIR during the planned shutdown and reconstruction periods of the GSI accelerator infrastructure.

The CRYRING coupled to the ESR is a powerful scientific instrument for research with cooled, highly-charged stable as well as exotic nuclides. For atomic physics, the low-energy highly-charged beams colliding with electrons and atoms of internal electron or gas targets will be used as a sensitive spectroscopic tool for the investigation of ionisation, recombination, excitation, and resonant scattering. It will also enable a range of experiments in nuclear and astrophysics as well as at the border between atomic and nuclear physics.

The combination of the ESR and the CRYRING is ideally suited for investigations of astrophysical capture reactions. The p-process Gamow window for capture reactions on nuclei in the tin region at $T_9 = 2 - 3$ is $E_{\mathrm{Gamow}} = 1.8 - 4.5$ MeV for proton- and $5.3 - 10.3$ MeV for α-induced reactions, which are perfectly within the energy range of the CRYRING [90]. These experiments, however, require the installation of particle detectors inside the ultra-high vacuum of the ring. The development of the corresponding detectors is ongoing.

9.3 Storage Rings at FAIR

A complex of several storage rings is planned at the future FAIR facility which is schematically illustrated in Figure 21.

It is proposed to extend the existing GSI facility by adding the heavy-ion synchrotrons SIS-100 and SIS-300, a two-stage large-acceptance supercon-

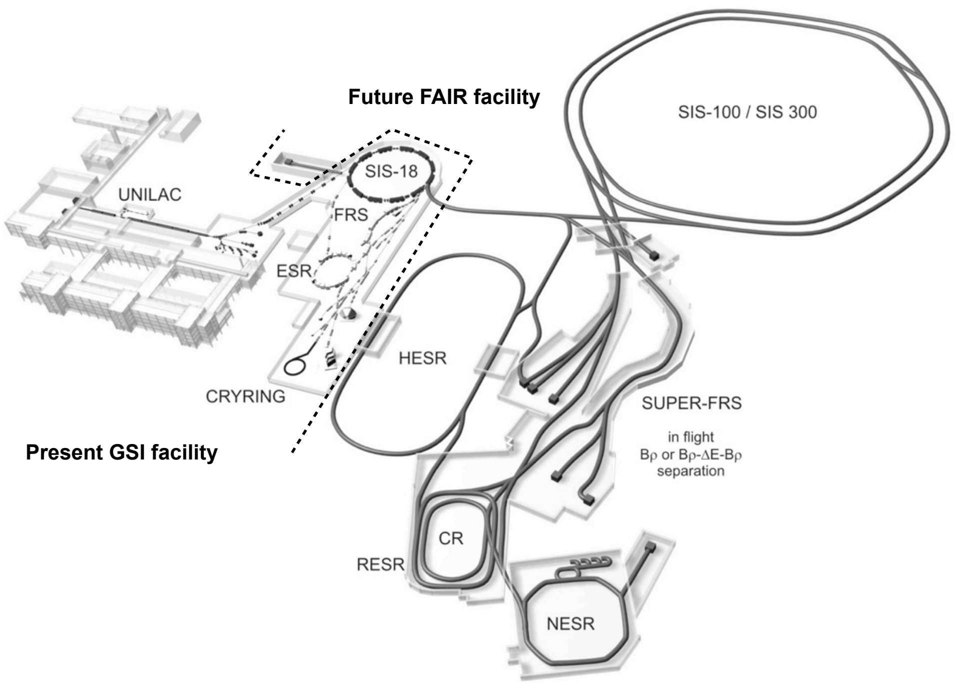

Fig. 21: A schematic view of the Facility for Antiproton and Ion Research in Darmstadt. The present GSI facility consisting of the UNILAC, SIS, FRS and ESR is shown together with the location of the CRYRING which is presently being reassembled.

ducting fragment separator Super-FRS [32] and a dedicated complex of storage rings (the Collector Ring (CR), the Recuperated Experimental Storage Ring (RESR), the New Experimental Storage Ring (NESR), and the High-Energy Storage Ring (HESR)). With the new storage rings, the option (a) in Figure 1 will significantly be extended.

It is envisioned that secondary beam intensities will be superior by about 4 orders of magnitude compared to those presently available. The exotic nuclei separated in-flight by the Super-FRS will be stochastically pre-cooled in the CR and transported via RESR to the NESR or HESR for in-ring experiments. However, FAIR will be realised in stages, which are defined by the Modularised Start Version of FAIR (MSV). The RESR and NESR rings are not part of the MSV and shall be constructed at a significantly later stage. Due to the MSV, the facility design was modified to enable its operation also without these rings. One of the consequences was that the present ESR will stay in operation until it is replaced by the NESR. In addition, see Fig. 7, the CRYRING, which was moved from Stockholm University to GSI, will be installed behind the ESR [42]. A beam line connecting the Super-FRS via CR with the ESR is envisaged as an extension of the MSV of FAIR. If constructed, it will be possible to study the most exotic nuclei provided by the Super-FRS also with detection setups at the ESR-CRYRING. The experimental conditions at FAIR will substantially improve qualitatively and quantitatively the research potential on the physics of exotic nuclei, and will allow for exploring new regions in the chart of the nuclides, of high interest for nuclear structure and astrophysics. Several scientific programmes are put forward at FAIR and are discussed in the following.

9.3.1 ILIMA: Isomeric beams, LIfetimes and MAsses

The ILIMA project is based on the successful mass and half-life measurements at the present ESR. The key facility here will be the CR, which is particularly designed for conducting IMS measurements [20]. The ion-optical matching of the Super-FRS and the CR will provide a close to unity transmission of the secondary beams. The CR will be equipped with two time-of-flight (ToF) detectors installed in one of the straight sections, which will enable in-ring velocity measurement of each particle. The latter is indispensable for correction of the non-isochronicity (see [86]). Employing the novel resonant Schottky detectors [55] will enable simultaneous broad-band mapping of nuclear masses and lifetimes by the SMS technique. In addition, heavy-ion detectors will be installed after dipole magnets in the CR. The mass surface that will become accessible in the CR is illustrated in Figure 17, where the smallest production rate of one stored ion per day is assumed.

In addition to the experiments in the CR, there are plans to use the CRYRING and the HESR. It is proposed to search for the NEEC process in the former, whereas the accumulation scheme in the latter will be used to achieve high intensities of long-lived highly-charged radionuclides. One striking example to be addressed is the measurement of the bound-state β^--decay of ^{205}Tl [90] (predicted $T_{1/2} \approx 1$ year), which is important for solar neutrino physics and astrophysics.

9.3.2 EXL: EXotic nuclei studied in Light-ion induced reactions at the NESR storage ring

The objective of the EXL-project, is to capitalise on light-ion induced direct reactions in inverse kinematics [38]. Due to their spin-isospin selectivity, light-ion induced direct reactions at intermediate to high energies are an indispensable tool in nuclear structure investigations. For many cases of direct reactions the essential nuclear structure information is deduced from high-resolution measurements at low-momentum transfer. This is in particular true for example for the investigation of nuclear matter distributions by elastic proton scattering at low q, for the investigation of giant monopole resonances by inelastic scattering at low q, and for the investigation of Gamow-Teller transitions by charge exchange reactions at low q. Because of the conditions of inverse kinematics in case of beams of unstable nuclei, low-momentum transfer measurements turn out to be an exclusive domain of storage ring experiments. Here luminosities are superior by orders of magnitude compared to experiments with external targets.

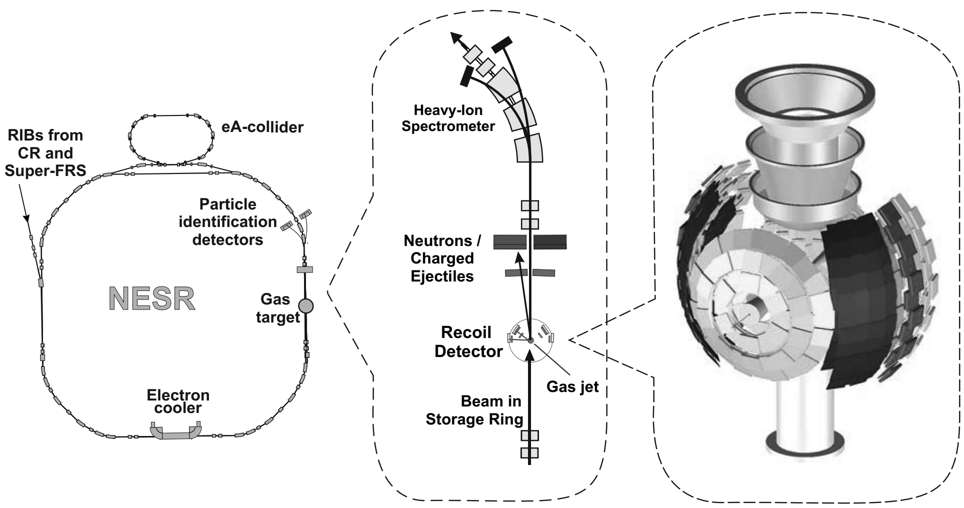

Fig. 22: Layout of the EXL setup at the NESR storage ring [37]. The left panel displays a view of the target recoil detector surrounding the internal gas-jet target (for details see text). Courtesy to Nasser Kalantar.

Within the EXL project the design of a complex detector setup was investigated with the aim to provide a highly efficient, high-resolution universal detection system, applicable to a wide class of nuclear reactions. It is schematically shown in Fig. 22. The apparatus is foreseen to be installed at the internal gas-jet target of the NESR storage cooler ring.

Since the NESR is not a part of the MSV of FAIR, the realisation of parts of the EXL project in the present ESR is discussed. Therefore, a transfer line from the CR to the ESR needs to be constructed such that the beams from the Super-FRS, pre-cooled in the CR, can become available also in the ESR.

9.3.3 ELISe: ELectron Ion Scattering in a Storage ring e-A collider

Electron scattering off nuclei provides a powerful tool for examining nuclear structure, which allows precision studies of nuclear properties like charge radii, density distributions, spectroscopic factors as well as giant resonances, etc. However, the electron scattering experiments are limited today to stable nuclear targets.

The ELISe project aims at elastic, inelastic and quasifree electron scattering, which will be possible for the first time for short lived nuclei [1]. It is proposed to construct an electron-ion collider at the NESR by using the intersecting ion and electron storage rings. For this purpose a small Electron and Antiproton Ring (EAR), eA collider in Figure 22, will be build which will store an intense electron beam (or an antiproton beam, see Section 9.3.4) . The scattered electrons will be analysed with a dedicated electron spectrometer with high resolution and large solid angle coverage, while the recoils will be analysed with particle detectors using the bending section of the NESR as a spectrometer. The investigation of charge densities, transition densities, single particle structure, etc. on nuclei far off stability will complement the investigations of the EXL project, and allow in many cases for a more complete and model independent information of the structure of such nuclei.

Similar to the EXL project, due to the delay in the construction of NESR, the feasibility to realise the ELISe project at the present ESR is being investigated. In this case, the ELISe project will also profit from the CR-ESR transfer line delivering secondary beams from the Super-FRS to the ESR.

9.3.4 AIC: The Antiproton-Ion-Collider at FAIR

One of the main capabilities of FAIR is the availability of intense antiproton beams in a wide range of energies. Within the AIC project, it is proposed to explore collisions of antiproton beams with beams of exotic nuclei, in order to measure simultaneously neutron and proton distributions [40]. Here, a modified EAR ring (see Section 9.3.3) can be used to store 30 MeV antiprotons. The antiprotons are brought into head-on collisions with relativistic exotic nuclei stored in the NESR at energies of up to 740 MeV/u. An antiproton can annihilate on a proton or a neutron of the studied nucleus.

This leads to different reaction-product nuclei which can unambiguously be identified after the reaction with Schottky spectrometry or particle detectors after the bending section of the NESR. Thus, an independent measurement of proton and neutron radii within the same experiment is possible.

The AIC project requires both, the NESR and EAR rings as well as the possibility to bring antiproton beams into the EAR. This complicates the transfer of the AIC project to the ESR for the time until the construction of NESR is completed, though various possibilities are presently being studied taking into account that the transport of antiprotons would be possible with the CR-ESR transfer line.

9.3.5 SPARC: The Stored Particle Atomic Research Collaboration at FAIR

The SPARC collaboration aims to exploit the multitude of new and challenging opportunities for atomic physics research at FAIR [74]. Relevant for this review, is the planned application of the atomic physics techniques to determine properties of stable and unstable nuclei. Thus, the measurements of isotopic shifts by employing laser spectroscopy or dielectronic recombination studies will allow the determination of nuclear magnetic moments, spins and radii.

The SPARC research programme was focused on the NESR, whose design was correspondingly optimised. The development of the required instrumentation and a significant part of the envisioned experiments are feasible in the present ESR, especially after the CRYRING will be constructed behind the ESR [42], and at the HESR [74]. In the latter case, due to the Doppler effect the laser spectroscopy studies will profit from the high kinetic energies by addressing transitions that are inaccessible otherwise.

9.4 High Intensity Heavy Ion Accelerator Facility

The concept for a new-generation heavy-ion accelerator facility in China, High Intensity Heavy Ion Accelerator Facility (HIAF), is being prepared at the IMP.

For the driver machine of this national user facility it is proposed to use a powerful superconducting linac, which shall be able to accelerate intense beams of all elements from protons to Uranium. The design of the HIAF is not finalised yet. However, it is envisioned to have a complex of several storage rings which are considered for a broad multidisciplinary research, like nuclear structure, astrophysics, atomic-, plasma-, accelerator-, and neutrino- physics, as well as investigations of fundamental symmetries and interactions, etc. It is emphasised, that a dedicated storage ring for isochronous mass measurements of shortest lived nuclides is envisioned.

10 Conclusion

The commissioning of the ESR in 1990 and the first exciting results at this facility resulted in a number of storage ring projects which were proposed worldwide. However, only the storage ring facility CSRe in Lanzhou was taken into operation in 2007 [91].

In the last two and a half decades, ion storage-cooler rings, fed by highly-charged radioactive nuclei, have been proven as excellent tools to study the ground state properties, such as masses and β-lifetimes, of these exotic nuclei. The dreams to conduct nuclear reactions in a storage ring were around ever since the ESR was taken into operation. The advantages of such studies are the inverse reaction kinematics, the brilliant quality of the cooled beams and the unique possibility to re-use many times the rare nuclear species for reactions with windowless thin internal targets. Now, the first reaction experiments were successfully conducted in the ESR.

This all led to an increased interest in in-ring experiments addressing nuclear structure and nuclear astrophysics questions, which is indicated by a number of new storage ring projects that were launched worldwide. These projects comprise facilities for storing beams at energies of 10 MeV/u and below (the storage ring project at HIE-ISOLDE and CRYRING at the ESR), at intermediate energies of a few hundreds of MeV/u (the CR, the RESR, the HESR and the RI-RING) and at high energies reaching 5 GeV/u and higher (the HESR and the high energy rings within the HIAF project in China). The highly-complementary physics programmes envisioned at these rings aim at exploiting the unique capabilities of the corresponding radioactive beam facilities and will undoubtedly provide new breathtaking results already in the near future.

Acknowledgements

This script is entirely based on the common publications with many colleagues working over many years on various storage ring experiments. Their help I greatly appreciate. This research is supported by the BMBF grant in the framework of the Internationale Zusammenarbeit in Bildung und Forschung Projekt-Nr. 01DO12012 by the Helmholtz-CAS Joint Research Group HCJRG-108, by the External Cooperation Program of the Chinese

Academy Sciences Grant No. GJHZ1305, and by the European Research Council through the Consolidator Grant ASTRUm (Project No. 682841). I thank the Chinese Academy of Sciences for support within the visiting professorship for senior international scientists program (Grant No.2009J2-23), and ESF for support within the Euro GENESIS program.

References

[1] A. Antonov, M. Gaidarov, M. Ivanov, D. Kadrev, M. Aiche, G. Barreau, S. Czajkowski, B. Jurado, G. Belier, A. Chatillon, T. Granier, J. Taieb, D. Dore, A. Letourneau, D. Ridikas, E. Dupont, E. Berthoumieux, S. Panebianco, F. Farget, C. Schmitt, L. Audouin, E. Khan, L. Tassan-Got, T. Aumann, P. Beller, K. Boretzky, A. Dolinskii, P. Egelhof, H. Emling, B. Franzke, H. Geissel, A. Kelic-Heil, O. Kester, N. Kurz, Y. Litvinov, G. Münzenberg, F. Nolden, K.-H. Schmidt, C. Scheidenberger, H. Simon, M. Steck, H. Weick, J. Enders, N. Pietralla, A. Richter, G. Schrieder, A. Zilges, M. Distler, H. Merkel, U. Müller, A. Junghans, H. Lenske, M. Fujiwara, T. Suda, S. Kato, T. Adachi, S. Hamieh, M. Harakeh, N. Kalantar-Nayestanaki, H. Wörtche, G. Berg, I. Koop, P. Logatchov, A. Otboev, V. Parkhomchuk, D. Shatilov, P. Shatunov, Y. Shatunov, S. Shiyankov, D. Shvartz, A. Skrinsky, L. Chulkov, B. Danilin, A. Korsheninnikov, E. Kuzmin, A. Ogloblin, V. Volkov, Y. Grishkin, V. Lisin, A. Mushkarenkov, V. Nedorezov, A. Polonski, N. Rudnev, A. Turinge, A. Artukh, V. Avdeichikov, S. Ershov, A. Fomichev, M. Golovkov, A. Gorshkov, L. Grigorenko, S. Klygin, S. Krupko, I. Meshkov, A. Rodin, Y. Sereda, I. Seleznev, S. Sidorchuk, E. Syresin, S. Stepantsov, G. Ter-Akopian, Y. Teterev, A. Vorontsov, S. Kamerdzhiev, E. Litvinova, S. Karataglidis, R. A. Rodriguez, M. Borge, C. F. Ramirez, E. Garrido, P. Sarriguren, J. Vignote, L. F. Prieto, J. L. Herraiz, E. M. de Guerra, J. Udias-Moinelo, J. A. Soriano, A. L. Rojo, J. Caballero, H. Johansson, B. Jonson, T. Nilsson, G. Nyman, M. Zhukov, P. Golubev, D. Rudolph, K. Hencken, J. Jourdan, B. Krusche, T. Rauscher, D. Kiselev, D. Trautmann, J. Al-Khalili, W. Catford, R. Johnson, P. Stevenson, C. Barton, D. Jenkins, R. Lemmon, M. Chartier, D. Cullen, C. Bertulani, and A. Heinz. The electron-ion scattering experiment elise at the international facility for antiproton and ion research (fair)a conceptual design study. *Nuclear Instruments and Methods in Physics Research Section A: Accelerators, Spectrometers, Detectors and Associated Equipment*, 637(1):60 – 76, 2011.

[2] P. Armbruster, H.-G. Clerc, J. P. Dufour, B. Franczak, H. Geissel, E. Hanelt, O. Klepper, B. Langenbeck, G. Münzenberg, F. Nickel, M. S. Pravikoff, E. Roeckl, D. Schardt, K.-H. Schmidt, D. Schüll, T. Schwab, B. Sherrill, K. Sümmerer, and H. Wollnik. The projectile-

fragment separator at the Darmstadt SIS/ESR facility. *AIP Conference Proceedings*, 164(1):839–844, 1987.

[3] D. R. Atanasov, N. Winckler, D. Balabanski, L. Batist, F. Bosch, D. Boutin, C. Brandau, C. Dimopoulou, H. G. Essel, T. Faestermann, H. Geissel, I. Hachiuma, S. Hess, T. Izumikawa, P. Kienle, R. Knöbel, C. Kozhuharov, J. Kurcewicz, N. Kuzminchuk, S. A. Litvinov, Y. A. Litvinov, R. S. Mao, R. Märtin, M. Mazzocco, G. Münzenberg, K. Namihira, F. Nolden, T. Ohtsubo, Z. Patyk, R. Reuschl, M. S. Sanjari, C. Scheidenberger, D. Shubina, U. Spillmann, M. Steck, T. Stöhlker, B. Sun, T. Suzuki, M. Trassinelli, I. I. Tupitsyn, H. Weick, M. Winkler, D. F. A. Winters, and T. Yamaguchi. Half-life measurements of stored fully ionized and hydrogen-like ^{122}I ions. *The European Physical Journal A*, 48(2):22, 2012.

[4] G. Audi, M. Wang, A. H. Wapstra, F. G. Kondev, M. MacCormick, X. Xu, and B. Pfeiffer. The AME2012 atomic mass evaluation (I). Evaluation of input data, adjustment procedures. *Chinese Physics C*, 36:1287–1602, 2012.

[5] M. Bernas, S. Czajkowski, P. Armbruster, H. Geissel, P. Dessagne, C. Donzaud, H.-R. Faust, E. Hanelt, A. Heinz, M. Hesse, C. Kozhuharov, C. Miehe, G. Münzenberg, M. Pfützner, C. Röhl, K.-H. Schmidt, W. Schwab, C. Stephan, K. Sümmerer, L. Tassan-Got, and B. Voss. Projectile fission at relativistic velocities: a novel and powerful source of neutron-rich isotopes well suited for in-flight isotopic separation. *Physics Letters B*, 331(1-2):19 – 24, 1994.

[6] H. F. Beyer, T. Gassner, M. Trassinelli, R. Heß, U. Spillmann, D. Bana, K.-H. Blumenhagen, F. Bosch, C. Brandau, W. Chen, C. Dimopoulou, E. Förster, R. E. Grisenti, A. Gumberidze, S. Hagmann, P.-M. Hillenbrand, P. Indelicato, P. Jagodzinski, T. Kämpfer, C. Kozhuharov, M. Lestinsky, D. Liesen, Y. A. Litvinov, R. Loetzsch, B. Manil, R. Märtin, F. Nolden, N. Petridis, M. S. Sanjari, K. S. Schulze, M. Schwemlein, A. Simionovici, M. Steck, T. Stöhlker, C. I. Szabo, S. Trotsenko, I. Uschmann, G. Weber, O. Wehrhan, N. Winckler, D. F. A. Winters, N. Winters, and E. Ziegler. Crystal optics for precision x-ray spectroscopy on highly charged ionsconception and proof. *Journal of Physics B: Atomic, Molecular and Optical Physics*, 48(14):144010, 2015.

[7] K. Blasche, D. Böhne, B. Franzke, and H. Prange. The SIS Heavy Ion Synchrotron Project. *IEEE Transactions on Nuclear Science*, NS-32(5):2657–2661, Oct. 1985.

[8] K. Blaum. High-accuracy mass spectrometry with stored ions. *Physics Reports*, 425(1):1–78, 2006.

[9] A. Bohr and B. Mottelson. *Nuclear Structure*. World Scientific, 1969.

[10] F. Bosch, T. Faestermann, J. Friese, F. Heine, P. Kienle, E. Wefers, K. Zeitelhack, K. Beckert, B. Franzke, O. Klepper, C. Kozhuharov, G. Menzel, R. Moshammer, F. Nolden, H. Reich, B. Schlitt, M. Steck, T. Stöhlker, T. Winkler, and K. Takahashi. Observation of bound-state β^- decay of fully ionized ^{187}re: ^{187}re$-^{187}$os cosmochronometry. *Phys. Rev. Lett.*, 77:5190–5193, Dec 1996.

[11] F. Bosch, H. Geissel, Y. Litvinov, K. Beckert, B. Franzke, M. Hausmann, T. Kerscher, O. Klepper, C. Kozhuharov, K. Löbner, G. Münzenberg, F. Nolden, Y. Novikov, Z. Patyk, T. Radon, C. Scheidenberger, M. Steck, and H. Wollnik. Experiments with stored exotic nuclei at relativistic energies. *International Journal of Mass Spectrometry*, 251(2-3):212–219, 2006.

[12] F. Bosch and Y. A. Litvinov. Mass and lifetime measurements at the experimental storage ring of {GSI}. *International Journal of Mass Spectrometry*, 349-350:151 – 161, 2013. 100 years of Mass Spectrometry.

[13] F. Bosch, Y. A. Litvinov, and T. Stöhlker. Nuclear physics with unstable ions at storage rings. *Progress in Particle and Nuclear Physics*, 73:84–140, 2013.

[14] B. Botermann, D. Bing, C. Geppert, G. Gwinner, T. W. Hänsch, G. Huber, S. Karpuk, A. Krieger, T. Kühl, W. Nörtershäuser, C. Novotny, S. Reinhardt, R. Sánchez, D. Schwalm, T. Stöhlker, A. Wolf, and G. Saathoff. Test of time dilation using stored li$^+$ ions as clocks at relativistic speed. *Phys. Rev. Lett.*, 113:120405, Sep 2014.

[15] C. Brandau, C. Kozhuharov, A. Müller, D. Bernhardt, F. Bosch, D. Boutin, F. J. Currell, C. Dimopoulou, B. Franzke, S. Fritzsche, A. Gumberidze, Z. Harman, U. D. Jentschura, C. H. Keitel, Y. S. Kozhedub, R. Krücken, Y. A. Litvinov, F. Nolden, B. O'Rourke, R. Reuschl, S. Schippers, V. M. Shabaev, U. Spillmann, Z. Stachura,

M. Steck, T. Stöhlker, I. I. Tupitsyn, D. F. A. Winters, and A. Wolf. Resonant recombination at ion storage rings: A conceptual alternative for isotope shift and hyperfine studies. *Hyperfine Interactions*, 196(1-3):115–127, 2010.

[16] L. Chen, Y. A. Litvinov, W. R. Plaß, K. Beckert, P. Beller, F. Bosch, D. Boutin, L. Caceres, R. B. Cakirli, J. J. Carroll, R. F. Casten, R. S. Chakrawarthy, D. M. Cullen, I. J. Cullen, B. Franzke, H. Geissel, J. Gerl, M. Górska, G. A. Jones, A. Kishada, R. Knöbel, C. Kozhuharov, S. A. Litvinov, Z. Liu, S. Mandal, F. Montes, G. Münzenberg, F. Nolden, T. Ohtsubo, Z. Patyk, Z. Podolyák, R. Propri, S. Rigby, N. Saito, T. Saito, C. Scheidenberger, M. Shindo, M. Steck, P. Ugorowski, P. M. Walker, S. Williams, H. Weick, M. Winkler, H.-J. Wollersheim, and T. Yamaguchi. Schottky mass measurement of the ^{208}Hg isotope: Implication for the proton-neutron interaction strength around doubly magic ^{208}Pb. *Phys. Rev. Lett.*, 102:122503, Mar 2009.

[17] L. Chen, W. R. Plass, H. Geissel, R. Knöbel, C. Kozhuharov, Y. A. Litvinov, Z. Patyk, C. Scheidenberger, K. Siegień-Iwaniuk, B. Sun, H. Weick, K. Beckert, P. Beller, F. Bosch, D. Boutin, L. Caceres, J. J. Carroll, D. M. Cullen, I. J. Cullen, B. Franzke, J. Gerl, M. Górska, G. A. Jones, A. Kishada, J. Kurcewicz, S. A. Litvinov, Z. Liu, S. Mandal, F. Montes, G. Münzenberg, F. Nolden, T. Ohtsubo, Z. Podolyák, R. Propri, S. Rigby, N. Saito, T. Saito, M. Shindo, M. Steck, P. Ugorowski, P. M. Walker, S. Williams, M. Winkler, H.-J. Wollersheim, and T. Yamaguchi. Discovery and investigation of heavy neutron-rich isotopes with time-resolved Schottky spectrometry in the element range from thallium to actinium. *Physics Letters B*, 691(5):234–237, 2010.

[18] D. T. Doherty, S. Kraft-Bermuth, and S. Litvinov. The "stori" of the rings 2014a summary of the stori14 conference. *Physica Scripta*, T166:014077, 2015.

[19] D. T. Doherty, P. J. Woods, Y. A. Litvinov, M. A. Najafi, S. Bagchi, S. Bishop, M. Bo, C. Brandau, T. Davinson, I. Dillmann, A. Estrade, P. Egelhof, A. Evdokimov, A. Gumberidze, M. Heil, C. Lederer, S. A. Litvinov, G. Lotay, N. Kalantar-Nayestanaki, O. Kiselev, C. Kozhuharov, T. Kröll, M. Mahjour-Shafei, M. Mutterer, F. Nolden, N. Petridis, U. Popp, R. Reifarth, C. Rigollet, S. Roy, M. Steck,

T. Stöhlker, B. Streicher, S. Trotsenko, M. von Schmid, X. L. Yan, and J. C. Zamora. Nuclear transfer reaction measurements at the esr for the investigation of the astrophysical $^{15}o(\alpha,\gamma)^{19}ne$ reaction. *Physica Scripta*, T166:014007, 2015.

[20] A. Dolinskii, D. Berkaev, U. Blell, C. Dimopoulou, O. Gorda, H. Leibrock, S. Litvinov, U. Laier, I. Koop, I. Schurig, A. Starostenko, P. Shatunov, and U. Weinrich. Collector ring project at fair. *Physica Scripta*, T166:014040, 2015.

[21] G. D. Dracoulis. Isomers, nuclear structure and spectroscopy. *Physica Scripta*, T152:014015, 2013.

[22] P. Egelhof, Y. A. Litvinov, and M. Steck, editors. *Physica Scripta*, volume T166. 2015.

[23] T. Enqvist, J. Benlliure, F. Farget, K.-H. Schmidt, P. Armbruster, M. Bernas, L. Tassan-Got, A. Boudard, R. Legrain, C. Volant, C. Böckstiegel, M. de Jong, and J. Dufour. Systematic experimental survey on projectile fragmentation and fission induced in collisions of 238u at 1 a gev with lead. *Nuclear Physics A*, 658(1):47 – 66, 1999.

[24] T. Enqvist, W. Wlazlo, P. Armbruster, J. Benlliure, M. Bernas, A. Boudard, S. Czajkowski, R. Legrain, S. Leray, B. Mustapha, M. Pravikoff, F. Rejmund, K.-H. Schmidt, C. Stephan, J. Taieb, L. Tassan-Got, and C. Volant. Isotopic yields and kinetic energies of primary residues in 1 a gev 208pb+p reactions. *Nuclear Physics A*, 686(1-4):481 – 524, 2001.

[25] B. Franzke. The heavy ion storage and cooler ring project ESR at GSI. *Nuclear Instruments and Methods in Physics Research Section B: Beam Interactions with Materials and Atoms*, 24/25:18–25, 1987.

[26] B. Franzke, H. Geissel, and G. Münzenberg. Mass and lifetime measurements of exotic nuclei in storage rings. *Mass Spectrometry Reviews*, 27(5):428–469, 2008.

[27] J.-J. Gaimard and K.-H. Schmidt. A reexamination of the abrasion-ablation model for the description of the nuclear fragmentation reaction. *Nuclear Physics A*, 531(3-4):709 – 745, 1991.

[28] H. Geissel, P. Armbruster, K. Behr, A. Brünle, K. Burkard, M. Chen, H. Folger, B. Franczak, H. Keller, O. Klepper, B. Langenbeck,

F. Nickel, E. Pfeng, M. Pfützner, E. Roeckl, K. Rykaczewski, I. Schall, D. Schardt, C. Scheidenberger, K.-H. Schmidt, A. Schröter, T. Schwab, K. Sümmerer, M. Weber, G. Münzenberg, T. Brohm, H.-G. Clerc, M. Fauerbach, J.-J. Gaimard, A. Grewe, E. Hanelt, B. Knödler, M. Steiner, B. Voss, J. Weckenmann, C. Ziegler, A. Magel, H. Wollnik, J. Dufour, Y. Fujita, D. Vieira, and B. Sherrill. The GSI projectile fragment separator (FRS): A versatile magnetic system for relativistic heavy ions. *Nuclear Instruments and Methods in Physics Research Section B: Beam Interactions with Materials and Atoms*, 70(1):286–297, 1992.

[29] H. Geissel, K. Beckert, F. Bosch, H. Eickhoff, B. Franczak, B. Franzke, M. Jung, O. Klepper, R. Moshammer, G. Münzenberg, F. Nickel, F. Nolden, U. Schaaf, C. Scheidenberger, P. Spädtke, M. Steck, K. Sümmerer, and A. Magel. First storage and cooling of secondary heavy-ion beams at relativistic energies. *Physical Review Letters*, 68:3412–3415, 1992.

[30] H. Geissel, Y. Litvinov, F. Attallah, K. Beckert, P. Beller, F. Bosch, D. Boutin, T. Faestermann, M. Falch, B. Franzke, M. Hausmann, M. Hellström, E. Kaza, T. Kerscher, O. Klepper, H.-J. Kluge, C. Kozhuharov, K.-L. Kratz, S. Litvinov, K. Löbner, L. Maier, M. Matoš, G. Münzenberg, F. Nolden, Y. Novikov, T. Ohtsubo, A. Ostrowski, Z. Patyk, B. Pfeiffer, M. Portillo, T. Radon, C. Scheidenberger, V. Shishkin, J. Stadlmann, M. Steck, D. Viera, H. Weick, M. Winkler, H. Wollnik, and T. Yamaguchi. New results with stored exotic nuclei at relativistic energies. *Nuclear Physics A*, 746:150c–155c, 2004.

[31] H. Geissel, G. Munzenberg, and K. Riisager. Secondary exotic nuclear beams. *Annual Review of Nuclear and Particle Sciences*, 45:163, 1995.

[32] H. Geissel, H. Weick, M. Winkler, G. Münzenberg, V. Chichkine, M. Yavor, T. Aumann, K. Behr, M. Böhmer, A. Brünle, K. Burkard, J. Benlliure, D. Cortina-Gil, L. Chulkov, A. Dael, J.-E. Ducret, H. Emling, B. Franczak, J. Friese, B. Gastineau, J. Gerl, R. Gernhäuser, M. Hellström, B. Jonson, J. Kojouharova, R. Kulessa, B. Kindler, N. Kurz, B. Lommel, W. Mittig, G. Moritz, C. Mühle, J. Nolen, G. Nyman, P. Roussell-Chomaz, C. Scheidenberger, K.-H. Schmidt, G. Schrieder, B. Sherrill, H. Simon, K. Sümmerer, N. Tahir, V. Vysotsky, H. Wollnik, and A. Zeller. The super-frs project at gsi. *Nuclear*

Instruments and Methods in Physics Research Section B: Beam Interactions with Materials and Atoms, 204:71 – 85, 2003.

[33] M. Grieser, Y. A. Litvinov, R. Raabe, K. Blaum, Y. Blumenfeld, P. A. Butler, F. Wenander, P. J. Woods, M. Aliotta, A. Andreyev, A. Artemyev, D. Atanasov, T. Aumann, D. Balabanski, A. Barzakh, L. Batist, A.-P. Bernardes, D. Bernhardt, J. Billowes, S. Bishop, M. Borge, I. Borzov, F. Bosch, A. J. Boston, C. Brandau, W. Catford, R. Catherall, J. Cederkäll, D. Cullen, T. Davinson, I. Dillmann, C. Dimopoulou, G. Dracoulis, C. E. Düllmann, P. Egelhof, A. Estrade, D. Fischer, K. Flanagan, L. Fraile, M. A. Fraser, S. J. Freeman, H. Geissel, J. Gerl, P. Greenlees, R. E. Grisenti, D. Habs, R. von Hahn, S. Hagmann, M. Hausmann, J. J. He, M. Heil, M. Huyse, D. Jenkins, A. Jokinen, B. Jonson, D. T. Joss, Y. Kadi, N. Kalantar-Nayestanaki, B. P. Kay, O. Kiselev, H.-J. Kluge, M. Kowalska, C. Kozhuharov, S. Kreim, T. Kröll, J. Kurcewicz, M. Labiche, R. C. Lemmon, M. Lestinsky, G. Lotay, X. W. Ma, M. Marta, J. Meng, D. Mücher, I. Mukha, A. Müller, A. S. J. Murphy, G. Neyens, T. Nilsson, C. Nociforo, W. Nörtershäuser, R. D. Page, M. Pasini, N. Petridis, N. Pietralla, M. Pfützner, Z. Podolyák, P. Regan, M. W. Reed, R. Reifarth, P. Reiter, R. Repnow, K. Riisager, B. Rubio, M. S. Sanjari, D. W. Savin, C. Scheidenberger, S. Schippers, D. Schneider, R. Schuch, D. Schwalm, L. Schweikhard, D. Shubina, E. Siesling, H. Simon, J. Simpson, J. Smith, K. Sonnabend, M. Steck, T. Stora, T. Stöhlker, B. Sun, A. Surzhykov, F. Suzaki, O. Tarasov, S. Trotsenko, X. L. Tu, P. van Duppen, C. Volpe, D. Voulot, P. M. Walker, E. Wildner, N. Winckler, D. F. A. Winters, A. Wolf, H. S. Xu, A. Yakushev, T. Yamaguchi, Y. J. Yuan, Y. H. Zhang, and K. Zuber. Storage ring at HIE – ISOLDE. Technical design report. *The European Physical Journal Special Topics*, 207(1):1–117, 2012.

[34] M. Hausmann, F. Attallah, K. Beckert, F. Bosch, A. Dolinskiy, H. Eickhoff, M. Falch, B. Franczak, B. Franzke, H. Geissel, T. Kerscher, O. Klepper, H.-J. Kluge, C. Kozhuharov, K. Löbner, G. Münzenberg, F. Nolden, Y. Novikov, T. Radon, H. Schatz, C. Scheidenberger, J. Stadlmann, M. Steck, T. Winkler, and H. Wollnik. First isochronous mass spectrometry at the experimental storage ring ESR. *Nuclear Instruments and Methods in Physics Research Section A: Accelerators, Spectrometers, Detectors and Associated Equipment*, 446:569–580, 2000.

[35] M. Jung, F. Bosch, K. Beckert, H. Eickhoff, H. Folger, B. Franzke, A. Gruber, P. Kienle, O. Klepper, W. Koenig, C. Kozhuharov, R. Mann, R. Moshammer, F. Nolden, U. Schaaf, G. Soff, P. Spädtke, M. Steck, T. Stöhlker, and K. Sümmerer. First observation of bound-state β^- decay. *Phys. Rev. Lett.*, 69:2164–2167, Oct 1992.

[36] K. P. Jungmann. Fundamental symmetries and interactionsselected topics. *Physica Scripta*, T166:014033, 2015.

[37] N. Kalantar-Nayestanaki, H. Moeini, M. Mahjour-Shafiei, F. Aksouh, K. Beckert, P. Beller, K. Boretzky, A. Chatillon, A. Corsi, P. Egelhof, H. Emling, G. Ickert, S. Ilieva, C. Kozhuharov, T. L. Bleis, X. C. L. Xuang, Y. Litvinov, K. Mahata, J. P. Meier, F. Nolden, U. Popp, H. Simon, M. Steck, T. Stöhlker, H. Weick, A. Zalite, O. Kiselev, J. Jourdan, D. Kiselev, D. Werthmüller, and S. Paschalis. First feasibility study for EXL with prototype detectors at the ESR and detector simulations. *International Journal of Modern Physics E*, 18(02):524–530, 2009.

[38] O. A. Kiselev and E. Collaboration. The exl project, recent results and future perspectives. *Physica Scripta*, 2015(T166):014004, 2015.

[39] U. Köster. Resonance ionization laser ion sources. *Nuclear Physics A*, 701(1-4):441 – 451, 2002.

[40] R. Krücken, F. Bosch, M. Cargnelli, L. Fabbietti, T. Faestemann, B. Franzke, H. Fuhrmann, R. S. Hayano, A. Hirtl, J. Homolka, P. Kienle, C. Kozhuharov, H. Lenske, Y. Litvinov, J. Marton, F. Nolden, P. Ring, Y. Shatunov, A. N. Skrinsky, K. Suzuki, V. A. Vostrikov, T. Yamaguchi, E. Widmann, S. Wycech, and J. Zmeskal. The antiproton-ion-collider at fair. *AIP Conference Proceedings*, 831(1):3–7, 2006.

[41] T. Kubo, D. Kameda, H. Suzuki, N. Fukuda, H. Takeda, Y. Yanagisawa, M. Ohtake, K. Kusaka, K. Yoshida, N. Inabe, T. Ohnishi, A. Yoshida, K. Tanaka, and Y. Mizoi. Bigrips separator and zerodegree spectrometer at riken ri beam factory. *Progress in Theoretical and Experimental Physics*, 2012:03C003, 2012.

[42] M. Lestinsky, A. Bräuning-Demian, H. Danared, M. Engström, W. Enders, S. Fedotova, B. Franzke, A. Heinz, F. Herfurth, A. Källberg, O. Kester, Y. Litvinov, M. Steck, D. Reistad, A. Simonsson, Ö. Skeppstedt, T. Stöhlker, G. Vorobjev, and the CRYRING@ESR working

group. Cryring@esr: present status and future research. *Physica Scripta*, T166:014075, 2015.

[43] Y. Litvinov, S. Bishop, K. Blaum, F. Bosch, C. Brandau, L. Chen, I. Dillmann, P. Egelhof, H. Geissel, R. Grisenti, S. Hagmann, M. Heil, A. Heinz, N. Kalantar-Nayestanaki, R. Knöbel, C. Kozhuharov, M. Lestinsky, X. Ma, T. Nilsson, F. Nolden, A. Ozawa, R. Raabe, M. Reed, R. Reifarth, M. Sanjari, D. Schneider, H. Simon, M. Steck, T. Stöhlker, B. Sun, X. Tu, T. Uesaka, P. Walker, M. Wakasugi, H. Weick, N. Winckler, P. Woods, H. Xu, T. Yamaguchi, Y. Yamaguchi, and Y. Zhang. Nuclear physics experiments with ion storage rings. *Nuclear Instruments and Methods in Physics Research Section B: Beam Interactions with Materials and Atoms*, 317, Part B:603–616, 2013.

[44] Y. Litvinov, F. Bosch, N. Winckler, D. Boutin, H. Essel, T. Faestermann, H. Geissel, S. Hess, P. Kienle, R. Knöbel, C. Kozhuharov, J. Kurcewicz, L. Maier, K. Beckert, P. Beller, C. Brandau, L. Chen, C. Dimopoulou, B. Fabian, A. Fragner, E. Haettner, M. Hausmann, S. Litvinov, M. Mazzocco, F. Montes, A. Musumarra, C. Nociforo, F. Nolden, W. Plass, A. Prochazka, R. Reda, R. Reuschl, C. Scheidenberger, M. Steck, T. Stöhlker, S. Torilov, M. Trassinelli, B. Sun, H. Weick, and M. Winkler. Observation of non-exponential orbital electron capture decays of hydrogen-like ^{140}Pr and ^{142}Pm ions. *Physics Letters B*, 664(3):162 – 168, 2008.

[45] Y. Litvinov, H. Geissel, Y. Novikov, Z. Patyk, T. Radon, C. Scheidenberger, F. Attallah, K. Beckert, F. Bosch, M. Falch, B. Franzke, M. Hausmann, T. Kerscher, O. Klepper, H.-J. Kluge, C. Kozhuharov, K. Löbner, G. Münzenberg, F. Nolden, M. Steck, and H. Wollnik. Precision experiments with time-resolved Schottky mass spectrometry. *Nuclear Physics A*, 734(0):473–476, 2004.

[46] Y. A. Litvinov, F. Attallah, K. Beckert, F. Bosch, D. Boutin, M. Falch, B. Franzke, H. Geissel, M. Hausmann, T. Kerscher, O. Klepper, H.-J. Kluge, C. Kozhuharov, K. E. G. Löbner, G. Münzenberg, F. Nolden, Y. N. Novikov, Z. Patyk, T. Radon, C. Scheidenberger, J. Stadlmann, M. Steck, M. B. Trzhaskovskaya, and H. Wollnik. Observation of a dramatic hindrance of the nuclear decay of isomeric states for fully ionized atoms. *Physics Letters B*, 573:80–85, 2003.

[47] Y. A. Litvinov and F. Bosch. Beta decay of highly charged ions. *Reports on Progress in Physics*, 74(1):016301, 2011.

[48] Y. A. Litvinov, F. Bosch, H. Geissel, J. Kurcewicz, Z. Patyk, N. Winckler, L. Batist, K. Beckert, D. Boutin, C. Brandau, L. Chen, C. Dimopoulou, B. Fabian, T. Faestermann, A. Fragner, L. Grigorenko, E. Haettner, S. Hess, P. Kienle, R. Knöbel, C. Kozhuharov, S. A. Litvinov, L. Maier, M. Mazzocco, F. Montes, G. Münzenberg, A. Musumarra, C. Nociforo, F. Nolden, M. Pfützner, W. R. Plaß, A. Prochazka, R. Reda, R. Reuschl, C. Scheidenberger, M. Steck, T. Stöhlker, S. Torilov, M. Trassinelli, B. Sun, H. Weick, and M. Winkler. Measurement of the β^+ and orbital electron-capture decay rates in fully ionized, hydrogenlike, and heliumlike ^{140}Pr ions. *Phys. Rev. Lett.*, 99:262501, Dec 2007.

[49] Y. A. Litvinov, F. Bosch, C. Kozhuharov, X. Ma, T. Stöhlker, N. Winckler, and T. Yamaguchi. At the borderline between atomic and nuclear physics: two-body -decay of highly charged ions. *Physica Scripta*, 2011(T144):014001, 2011.

[50] M. Lochmann, R. Jöhren, C. Geppert, Z. Andelkovic, D. Anielski, B. Botermann, M. Bussmann, A. Dax, N. Frömmgen, M. Hammen, V. Hannen, T. Kühl, Y. A. Litvinov, R. López-Coto, T. Stöhlker, R. C. Thompson, J. Vollbrecht, A. Volotka, C. Weinheimer, W. Wen, E. Will, D. Winters, R. Sánchez, and W. Nörtershäuser. Observation of the hyperfine transition in lithium-like bismuth $^{209}\mathrm{Bi}^{80+}$: Towards a test of qed in strong magnetic fields. *Phys. Rev. A*, 90:030501, Sep 2014.

[51] B. Mei, T. Aumann, S. Bishop, K. Blaum, K. Boretzky, F. Bosch, C. Brandau, H. Bräuning, T. Davinson, I. Dillmann, C. Dimopoulou, O. Ershova, Z. Fülöp, H. Geissel, J. Glorius, G. Gyürky, M. Heil, F. Käppeler, A. Kelic-Heil, C. Kozhuharov, C. Langer, T. Le Bleis, Y. Litvinov, G. Lotay, J. Marganiec, G. Münzenberg, F. Nolden, N. Petridis, R. Plag, U. Popp, G. Rastrepina, R. Reifarth, B. Riese, C. Rigollet, C. Scheidenberger, H. Simon, K. Sonnabend, M. Steck, T. Stöhlker, T. Szücs, K. Sümmerer, G. Weber, H. Weick, D. Winters, N. Winters, P. Woods, and Q. Zhong. First measurement of the $^{96}\mathrm{Ru}(p,\gamma)^{97}\mathrm{Rh}$ cross section for the p process with a storage ring. *Phys. Rev. C*, 92:035803, Sep 2015.

[52] I. Meshkov. Storage and cooling of ion beams. *Physica Scripta*, T166:014037, 2015.

[53] D. R. Miller, R. C. Thompson, and B. B. Cunningham. Products of high energy deuteron and helium ion bombardments of copper. *Phys. Rev.*, 74:347–348, Aug 1948.

[54] F. Nolden, K. Beckert, P. Beller, B. Franzke, C. Peschke, and M. Steck. Experience and prospects of stochastic cooling of radioactive beams at GSI. *Nuclear Instruments and Methods in Physics Research Section A*, 532:329, 2004.

[55] F. Nolden, P. Hülsmann, Y. Litvinov, P. Moritz, C. Peschke, P. Petri, M. Sanjari, M. Steck, H. Weick, J. Wu, Y. Zang, S. Zhang, and T. Zhao. A fast and sensitive resonant Schottky pick-up for heavy ion storage rings. *Nuclear Instruments and Methods in Physics Research Section A: Accelerators, Spectrometers, Detectors and Associated Equipment*, 659:69–77, 2011.

[56] W. Nörtershäuser and R. Sanchez. Laser spectroscopy at storage rings. *Physica Scripta*, T166:014020, 2015.

[57] T. Ohtsubo, F. Bosch, H. Geissel, L. Maier, C. Scheidenberger, F. Attallah, K. Beckert, P. Beller, D. Boutin, T. Faestermann, B. Franczak, B. Franzke, M. Hausmann, M. Hellström, E. Kaza, P. Kienle, O. Klepper, H.-J. Kluge, C. Kozhuharov, Y. A. Litvinov, M. Matos, G. Münzenberg, F. Nolden, Y. N. Novikov, M. Portillo, T. Radon, J. Stadlmann, M. Steck, T. Stöhlker, K. Sümmerer, K. Takahashi, H. Weick, M. Winkler, and T. Yamaguchi. Simultaneous measurement of β^- decay to bound and continuum electron states. *Phys. Rev. Lett.*, 95:052501, Jul 2005.

[58] A. Ozawa, T. Uesaka, M. Wakasugi, and the Rare-RI Ring Collaboration. The rare-ri ring. *Progress of Theoretical and Experimental Physics*, 2012(1), 2012.

[59] Z. Patyk, H. Geissel, Y. A. Litvinov, A. Musumarra, and C. Nociforo. α-decay half-lives for neutral atoms and bare nuclei. *Phys. Rev. C*, 78:054317, Nov 2008.

[60] M. Petrick, W. Plaß, K.-H. Behr, A. Brünle, L. Caceres, J. Clark, Z. Di, S. Elisseev, M. Facina, A. Fettouhi, H. Geissel, W. Hüller, M. Huyse, C. Karagiannis, B. Kindler, R. Knöbel, Y. Kudryavtsev, J. Kurcewicz, T. Levant, Y. Litvinov, B. Lommel, M. Maier, D. Morrissey, G. Münzenberg, M. Portillo, G. Savard, C. Scheidenberger,

P. V. Duppen, H. Weick, M. Winkler, and B. Zabransky. Online test of thefrs ion catcher at gsi. *Nuclear Instruments and Methods in Physics Research Section B: Beam Interactions with Materials and Atoms*, 266(19-20):4493 – 4497, 2008.

[61] T. Radon, H. Geissel, G. Münzenberg, B. Franzke, T. Kerscher, F. Nolden, Y. Novikov, Z. Patyk, C. Scheidenberger, F. Attallah, K. Beckert, T. Beha, F. Bosch, H. Eickhoff, M. Falch, Y. Fujita, M. Hausmann, F. Herfurth, H. Irnich, H. Jung, O. Klepper, C. Kozhuharov, Y. Litvinov, K. Löbner, F. Nickel, H. Reich, W. Schwab, B. Schlitt, M. Steck, K. Sümmerer, T. Winkler, and H. Wollnik. Schottky mass measurements of stored and cooled neutron-deficient projectile fragments in the element range of 57z84. *Nuclear Physics A*, 677(1-4):75 – 99, 2000.

[62] T. Radon, T. Kerscher, B. Schlitt, K. Beckert, T. Beha, F. Bosch, H. Eickhoff, B. Franzke, Y. Fujita, H. Geissel, M. Hausmann, H. Irnich, H. C. Jung, O. Klepper, H.-J. Kluge, C. Kozhuharov, G. Kraus, K. E. G. Löbner, G. Münzenberg, Y. Novikov, F. Nickel, F. Nolden, Z. Patyk, H. Reich, C. Scheidenberger, W. Schwab, M. Steck, K. Sümmerer, and H. Wollnik. Schottky mass measurements of cooled proton-rich nuclei at the GSI experimental storage ring. *Phys. Rev. Lett.*, 78:4701–4704, 1997.

[63] M. W. Reed, I. J. Cullen, P. M. Walker, Y. A. Litvinov, K. Blaum, F. Bosch, C. Brandau, J. J. Carroll, D. M. Cullen, A. Y. Deo, B. Detwiller, C. Dimopoulou, G. D. Dracoulis, F. Farinon, H. Geissel, E. Haettner, M. Heil, R. S. Kempley, R. Knöbel, C. Kozhuharov, J. Kurcewicz, N. Kuzminchuk, S. Litvinov, Z. Liu, R. Mao, C. Nociforo, F. Nolden, W. R. Plass, A. Prochazka, C. Scheidenberger, M. Steck, T. Stöhlker, B. Sun, T. P. D. Swan, G. Trees, H. Weick, N. Winckler, M. Winkler, P. J. Woods, and T. Yamaguchi. Discovery of highly excited long-lived isomers in neutron-rich hafnium and tantalum isotopes through direct mass measurements. *Physical Review Letters*, 105:172501, 2010.

[64] M. W. Reed, P. M. Walker, I. J. Cullen, Y. A. Litvinov, K. Blaum, F. Bosch, C. Brandau, J. J. Carroll, D. M. Cullen, A. Y. Deo, B. Detwiler, C. Dimopoulou, G. D. Dracoulis, F. Farinon, H. Geissel, E. Haettner, M. Heil, R. S. Kempley, R. Knöbel, C. Kozhuharov, J. Kurcewicz, N. Kuzminchuk, S. Litvinov, Z. Liu, R. Mao, C. Nocif-

oro, F. Nolden, W. R. Plass, A. Prochazka, C. Scheidenberger, D. Shubina, M. Steck, T. Stöhlker, B. Sun, T. P. D. Swan, G. Trees, H. Weick, N. Winckler, M. Winkler, P. J. Woods, and T. Yamaguchi. Technique for resolving low-lying isomers in the experimental storage ring (ESR) forand the occurrence of an isomeric state in ^{192}Re. *Journal of Physics: Conference Series*, 381:2058, 2012.

[65] M. W. Reed, P. M. Walker, I. J. Cullen, Y. A. Litvinov, D. Shubina, G. D. Dracoulis, K. Blaum, F. Bosch, C. Brandau, J. J. Carroll, D. M. Cullen, A. Y. Deo, B. Detwiler, C. Dimopoulou, G. X. Dong, F. Farinon, H. Geissel, E. Haettner, M. Heil, R. S. Kempley, R. Knöbel, C. Kozhuharov, J. Kurcewicz, N. Kuzminchuk, S. Litvinov, Z. Liu, R. Mao, C. Nociforo, F. Nolden, W. R. Plass, Z. Podolyak, A. Prochazka, C. Scheidenberger, M. Steck, T. Stöhlker, B. Sun, T. P. D. Swan, G. Trees, H. Weick, N. Winckler, M. Winkler, P. J. Woods, F. R. Xu, and T. Yamaguchi. Long-lived isomers in neutron-rich $Z = 72 - 76$ nuclides. *Physical Review C*, 86:054321, 2012.

[66] B. Rossi. Über die eigenschaften der durchdringenden korpuskularstrahlung im meeresniveau. *Zeitschrift für Physik*, 82(3-4):151–178, 1933.

[67] R. Sanchez, J. Ullmann, J. Vollbrecht, Z. Andelkovic, A. Dax, W. Geithner, C. Geppert, C. Gorges, M. Hammen, V. Hannen, S. Kaufmann, K. König, Y. A. Litvinov, M. Lochmann, B. Maaå, J. Meisner, T. Murböck, W. Nörtershäuser, S. Schmidt, M. Schmidt, M. Steck, T. Stöhlker, R. C. Thompson, and C. Weinheimer. Hyperfine transition in 209 bi 80+ one step forward. *Physica Scripta*, T166:014021, 2015.

[68] H. Schatz, A. Aprahamian, V. Barnard, L. Bildsten, A. Cumming, M. Ouellette, T. Rauscher, F.-K. Thielemann, and M. Wiescher. End point of the *rp* process on accreting neutron stars. *Phys. Rev. Lett.*, 86:3471–3474, Apr 2001.

[69] C. Scheidenberger, K. Beckert, P. Beller, F. Bosch, C. Brandau, D. Boutin, L. Chen, B. Franzke, H. Geissel, R. Knöbel, C. Kozhuharov, J. Kurcewicz, S. Litvinov, Y. Litvinov, M. Mazzocco, G. Münzenberg, F. Nolden, W. Plaß, M. Steck, B. Sun, H. Weick, and M. Winkler. Isobar separation at frs-esr - a development towards pure isomeric stored beams. *Hyperfine Interactions*, 173(1-3):61–66, 2006.

[70] C. Scheidenberger, T. Stöhlker, W. Meyerhof, H. Geissel, P. Mokler, and B. Blank. Charge states of relativistic heavy ions in matter. *Nuclear Instruments and Methods in Physics Research Section B: Beam Interactions with Materials and Atoms*, 142(4):441 – 462, 1998.

[71] D. Shubina, R. B. Cakirli, Y. A. Litvinov, K. Blaum, C. Brandau, F. Bosch, J. J. Carroll, R. F. Casten, D. M. Cullen, I. J. Cullen, A. Y. Deo, B. Detwiler, C. Dimopoulou, F. Farinon, H. Geissel, E. Haettner, M. Heil, R. S. Kempley, C. Kozhuharov, R. Knöbel, J. Kurcewicz, N. Kuzminchuk, S. A. Litvinov, Z. Liu, R. Mao, C. Nociforo, F. Nolden, Z. Patyk, W. R. Plass, A. Prochazka, M. W. Reed, M. S. Sanjari, C. Scheidenberger, M. Steck, T. Stöhlker, B. Sun, T. P. D. Swan, G. Trees, P. M. Walker, H. Weick, N. Winckler, M. Winkler, P. J. Woods, T. Yamaguchi, and C. Zhou. Schottky mass measurements of heavy neutron-rich nuclides in the element range $70 \leq z \leq 79$ at the gsi experimental storage ring. *Phys. Rev. C*, 88:024310, Aug 2013.

[72] A. Sobiczewski and Y. A. Litvinov. Accuracy of theoretical descriptions of nuclear masses. *Phys. Rev. C*, 89:024311, Feb 2014.

[73] M. Steck, K. Beckert, H. Eickhoff, B. Franzke, F. Nolden, H. Reich, B. Schlitt, and T. Winkler. Anomalous Temperature Reduction of Electron-Cooled Heavy Ion Beams in the Storage Ring ESR. *Phys. Rev. Lett.*, 77:3803, 1996.

[74] T. Stöhlker, V. Bagnoud, K. Blaum, A. Blazevic, A. Bräuning-Demian, M. Durante, F. Herfurth, M. Lestinsky, Y. Litvinov, S. Neff, R. Pleskac, R. Schuch, S. Schippers, D. Severin, A. Tauschwitz, C. Trautmann, D. Varentsov, and E. Widmann. Appa at fair: From fundamental to applied research. *Nuclear Instruments and Methods in Physics Research Section B: Beam Interactions with Materials and Atoms*, 365, Part B:680 – 685, 2015.

[75] K. Sümmerer. Improved empirical parametrization of fragmentation cross sections. *Phys. Rev. C*, 86:014601, Jul 2012.

[76] K. Sümmerer and B. Blank. Modified empirical parametrization of fragmentation cross sections. *Phys. Rev. C*, 61:034607, Feb 2000.

[77] B. Sun, F. Bosch, D. Boutin, C. Brandau, L. Chen, C. Dimopoulou, B. Fabian, H. Geissel, R. Knöbel, C. Kozhuharov, J. Kurcewicz,

S. A. Litvinov, Y. A. Litvinov, J. Meng, G. Münzenberg, C. Nociforo, F. Nolden, W. R. Plaß, C. Scheidenberger, M. Steck, P. M. Walker, H. Weick, N. Winckler, and M. Winkler. Precise measurement of nuclear isomers in the storage ring at GSI. *Nuclear Physics A*, 834(1-4):476c–478c, 2010.

[78] B. Sun, R. Knöbel, H. Geissel, Y. Litvinov, P. Walker, K. Blaum, F. Bosch, D. Boutin, C. Brandau, L. Chen, I. Cullen, A. Dolinskii, B. Fabian, M. Hausmann, C. Kozhuharov, J. Kurcewicz, S. Litvinov, Z. Liu, M. Mazzocco, J. Meng, F. Montes, G. Münzenberg, A. Musumarra, S. Nakajima, C. Nociforo, F. Nolden, T. Ohtsubo, A. Ozawa, Z. Patyk, W. Plass, C. Scheidenberger, M. Steck, T. Suzuki, H. Weick, N. Winckler, M. Winkler, and T. Yamaguchi. Direct measurement of the 4.6 MeV isomer in stored bare ^{133}Sb ions. *Physics Letters B*, 688:294–297, 2010.

[79] B. Sun, Y. A. Litvinov, P. M. Walker, K. Beckert, P. Beller, F. Bosch, D. Boutin, C. Brandau, L. Chen, C. Dimopoulou, H. Geissel, R. K. Knöbel, C. Kozhuharov, J. Kurcewicz, S. A. Litvinov, M. Mazzocco, J. Meng, C. Nociforo, F. Nolden, W. R. Plass, C. Scheidenberger, M. Steck, H. Weick, and M. Winkler. Discovery of a new long-lived isomeric state in ^{125}Ce. *The European Physical Journal A*, 31(3):393, 2007.

[80] S. Tashenov, D. Banaś, H. Beyer, C. Brandau, S. Fritzsche, A. Gumberidze, S. Hagmann, P.-M. Hillenbrand, H. Jörg, I. Kojouharov, C. Kozhuharov, M. Lestinsky, Y. A. Litvinov, A. V. Maiorova, H. Schaffner, V. M. Shabaev, U. Spillmann, T. Stöhlker, A. Surzhykov, and S. Trotsenko. Observation of coherence in the time-reversed relativistic photoelectric effect. *Phys. Rev. Lett.*, 113:113001, Sep 2014.

[81] J. Thomson. XIX. Further experiments on positive rays. *Philosophical Magazine Series 6*, 24(140):209–253, 1912.

[82] J. Trötscher, K. Balog, H. Eickhoff, B. Franczak, B. Franzke, Y. Fujita, H. Geissel, C. Klein, J. Knollmann, A. Kraft, K. Löbner, A. Magel, G. Münzenberg, A. Przewloka, D. Rosenauer, H. Schäfer, M. Sendor, D. Vieira, B. Vogel, T. Winkelmann, and H. Wollnik. Mass measurements of exotic nuclei at the ESR. *Nuclear Instruments and Methods in Physics Research Section B: Beam Interactions with Materials and Atoms*, 70:455–458, 1992.

[83] M. von Schmid, S. Bagchi, S. Bönig, M. Csatls, I. Dillmann, C. Dimopoulou, P. Egelhof, V. Eremin, T. Furuno, H. Geissel, R. Gernhäuser, M. N. Harakeh, A.-L. Hartig, S. Ilieva, N. Kalantar-Nayestanaki, O. Kiselev, H. Kollmus, C. Kozhuharov, A. Krasznahorkay, T. Kröll, M. Kuilman, S. Litvinov, Y. A. Litvinov, M. Mahjour-Shafiei, M. Mutterer, D. Nagae, M. A. Najafi, C. Nociforo, F. Nolden, U. Popp, C. Rigollet, S. Roy, C. Scheidenberger, M. Steck, B. Streicher, L. Stuhl, M. Thürauf, T. Uesaka, H. Weick, J. S. Winfield, D. Winters, P. J. Woods, T. Yamaguchi, K. Yue, J. C. Zamora, J. Zenihiro, and the EXL collaboration. Investigation of the nuclear matter distribution of 56 ni by elastic proton scattering in inverse kinematics. *Physica Scripta*, T166:014005, 2015.

[84] M. Wakasugi and the RIKEN RI Ring Collaboration. The rare ri ring facility at the riken ri beam factory. *JPS Conference Proceedings*, 6:010020, 2015.

[85] P. Walker and G. Dracoulis. Energy traps in atomic nuclei. *Nature*, 399(6731):35–40, May 1999.

[86] P. Walker, Y. A. Litvinov, and H. Geissel. The ilima project at fair. *International Journal of Mass Spectrometry*, 349-350:247 – 254, 2013.

[87] R. K. Wallace and S. E. Woosley. Explosive hydrogen burning. *The Astrophysical Journal Supplement Series*, 45:389–420, 1981.

[88] N. Winckler, H. Geissel, Y. Litvinov, K. Beckert, F. Bosch, D. Boutin, C. Brandau, L. Chen, C. Dimopoulou, H. Essel, B. Fabian, T. Faestermann, A. Fragner, E. Haettner, S. Hess, P. Kienle, R. Knöbel, C. Kozhuharov, S. Litvinov, M. Mazzocco, F. Montes, G. Münzenberg, C. Nociforo, F. Nolden, Z. Patyk, W. Plass, A. Prochazka, R. Reda, R. Reuschl, C. Scheidenberger, M. Steck, T. Stöhlker, S. Torilov, M. Trassinelli, B. Sun, H. Weick, and M. Winkler. Orbital electron capture decay of hydrogen- and helium-like ^{142}Pm ions. *Physics Letters B*, 679(1):36 – 40, 2009.

[89] D. Winters, T. Beck, G. Birkl, C. Dimopoulou, V. Hannen, T. Kühl, M. Lochmann, M. Loeser, X. Ma, F. Nolden, W. Nörtershäuser, B. Rein, R. Snchez, U. Schramm, M. Siebold, P. Spiller, M. Steck, T. Stöhlker, J. Ullmann, T. Walther, W. Wen, J. Yang, D. Zhang, and M. Bussmann. Laser cooling of relativistic heavy-ion beams for fair. *Physica Scripta*, 2015(T166):014048, 2015.

[90] P. Woods, K. Blaum, F. Bosch, M. Heil, Y. A. Litvinov, and R. Reifarth. Nuclear astrophysics experiments at storage rings: midterm perspectives at gsi. *Physica Scripta*, T166:014002, 2015.

[91] J. Xia, W. Zhan, B. Wei, Y. Yuan, M. Song, W. Zhang, X. Yang, P. Yuan, D. Gao, H. Zhao, X. Yang, G. Xiao, K. Man, J. Dang, X. Cai, Y. Wang, J. Tang, W. Qiao, Y. Rao, Y. He, L. Mao, and Z. Zhou. The heavy ion cooler-storage-ring project (HIRFL − CSR) at Lanzhou. *Nuclear Instruments and Methods in Physics Research Section A: Accelerators, Spectrometers, Detectors and Associated Equipment*, 488:11–25, 2002.

[92] G. Q. Xiao, J. W. Xia, Y. J. Yuan, R. S. Mao, J. H. Zheng, X. L. Tu, M. Wang, W. X. Huang, H. S. Xu, and W. L. Zhan. Overview on the HIRFL − CSR facility. *International Journal of Modern Physics E*, 18(02):405, 2009.

[93] H. Xu. HIRFL − CSR physics program. *International Journal of Modern Physics E*, 18(02):335, 2009.

[94] H. Xu, Y. Zhang, and Y. A. Litvinov. Accurate mass measurements of exotic nuclei with the csre in lanzhou. *International Journal of Mass Spectrometry*, 349-350:162–171, Sept. 2013.

[95] X. L. Yan, F. Bosch, Y. A. Litvinov, F. Nolden, M. Steck, X. L. Tu, H. S. Xu, X. H. Zhou, and Y. H. Zhang. Investigation of the momentum compaction factor of the esr thorough schottky mass measurements. *Physica Scripta*, T166:014045, 2015.

[96] X. L. Yan, H. S. Xu, Y. A. Litvinov, Y. H. Zhang, H. Schatz, X. L. Tu, K. Blaum, X. H. Zhou, B. H. Sun, J. J. He, Y. Sun, M. Wang, Y. J. Yuan, J. W. Xia, J. C. Yang, G. Audi, G. B. Jia, Z. G. Hu, X. W. Ma, R. S. Mao, B. Mei, P. Shuai, Z. Y. Sun, S. T. Wang, G. Q. Xiao, X. Xu, T. Yamaguchi, Y. Yamaguchi, Y. D. Zang, H. W. Zhao, T. C. Zhao, W. Zhang, and W. L. Zhan. Mass measurement of ^{45}Cr and its impact on the Ca − Sc cycle in X-ray bursts. *The Astrophysical Journal Letters*, 766(1):L8, 2013.

[97] Y. Yuan, J. Yang, J. Xia, P. Yuan, W. Qiao, D. Gao, G. Xiao, H. Zhao, H. Xu, M. Song, X. Yang, X. Cai, L. Ma, X. Yang, K. Man, Y. He, Z. Zhou, J. Zhang, Z. Xu, Y. Liu, R. Mao, W. Zhang, D. Xie, L. Sun, Y. Yang, D. Yin, P. Li, J. Li, J. Shi, W. Chai, B. Wei, and W. Zhan.

Status of the hirfl-csr complex. *Nuclear Instruments and Methods in Physics Research Section B: Beam Interactions with Materials and Atoms*, 317, Part B:214–217, 2013.

[98] J. C. Zamora, S. Bagchi, S. Bönig, M. Csatls, I. Dillmann, C. Dimopoulou, P. Egelhof, V. Eremin, T. Furuno, H. Geissel, R. Gernhäuser, M. N. Harakeh, A.-L. Hartig, S. Ilieva, N. Kalantar-Nayestanaki, O. Kiselev, K. Kollmus, C. Kozhuharov, A. Krasznahorkay, T. Kröll, M. Kuilman, S. Litvinov, Y. A. Litvinov, M. Mahjour-Shafiei, M. Mutterer, D. Nagae, M. A. Najafi, C. Nociforo, F. Nolden, U. Popp, C. Rigollet, S. Roy, C. Scheidenberger, M. von Schmid, M. Steck, B. Streicher, L. Stuhl, M. Thürauf, T. Uesaka, H. Weick, J. S. Winfield, D. Winters, P. J. Woods, T. Yamaguchi, K. Yue, J. Zenihiro, and the EXL collaboration. Isoscalar giant resonance studies in a stored-beam experiment within exl. *Physica Scripta*, T166:014006, 2015.

[99] W. Zhan, H. Xu, G. Xiao, J. Xia, H. Zhao, and Y. Yuan. Progress in HIRFL − CSR. *Nuclear Physics A*, 834:694c–700c, 2010.

[100] Y. Zhang, Y. A. Litvinov, T. Uesaka, and H. Xu. Storage ring mass spectrometry for nuclear structure and astrophysics research. *Physica Scripta*, page in press, 2016.

[101] Y. H. Zhang, H. S. Xu, Y. A. Litvinov, X. L. Tu, X. L. Yan, S. Typel, K. Blaum, M. Wang, X. H. Zhou, Y. Sun, B. A. Brown, Y. J. Yuan, J. W. Xia, J. C. Yang, G. Audi, X. C. Chen, G. B. Jia, Z. G. Hu, X. W. Ma, R. S. Mao, B. Mei, P. Shuai, Z. Y. Sun, S. T. Wang, G. Q. Xiao, X. Xu, T. Yamaguchi, Y. Yamaguchi, Y. D. Zang, H. W. Zhao, T. C. Zhao, W. Zhang, and W. L. Zhan. Mass measurements of the neutron-deficient ^{41}Ti, ^{45}Cr, ^{49}Fe, and ^{53}Ni nuclides: First test of the isobaric multiplet mass equation in fp-shell nuclei. *Phys. Rev. Lett.*, 109:102501, Sep 2012.

[102] Q. Zhong, T. Aumann, S. Bishop, K. Blaum, K. Boretzky, F. Bosch, H. Bräuning, C. Brandau, T. Davinson, I. Dillmann, O. Ershova, H. Geissel, G. Gyürky, M. Heil, F. Käppeler, A. Kelić, C. Kozhuharov, C. Langer, T. L. Bleis, Y. A. Litvinov, G. Lotay, J. Marganiec, N. Petridis, R. Plag, U. Popp, R. Reifarth, B. Riese, C. Rigollet, C. Scheidenberger, H. Simon, T. Stöhlker, T. Szücs, G. Weber, H. Weick, D. F. A. Winters, N. Winters, and P. J. Woods. ^{96}Ru$(p,\gamma)^{97}$Rh

measurement at the GSI storage ring. *Journal of Physics: Conference Series*, 202:2011, 2010.